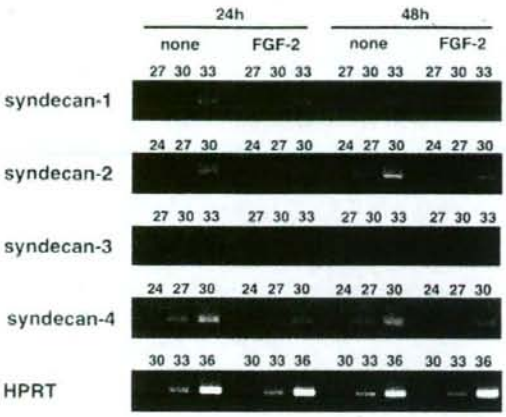

Fig. 4. mRNA expression of the syndecan gene family in HPDL cells. The expression of mRNA of the syndecan gene family in HPDL cells cultured in the absence or presence of FGF-2 (50 ng/ml) for 24 h and 48 h was measured. Total RNA was recovered and RT-PCR performed to analyze the mRNA expression of syndecan-1, -2, -3, and -4, and HPRT in HPDL cells. Results of one representative experiment from three separate experiments are shown. The number of PCR amplification cycles is shown above each lane.

between 48 and 72 h being particularly pronounced. In addition, the amount of HS produced was dependent on the dose of FGF-2 (Fig. 1).

The effects of other cytokines on the production of HS were then investigated, as production of HS can be modulated by various factors. In contrast to the marked effect of FGF-2, PDGF-BB slightly stimulated and TGF-β weakly suppressed the production of HS by HPDL cells, and the other cytokines examined (EGF, HGF, and IGF-1) did not alter HS production (Fig. 2). However, minor effects of PDGF-BB and TGF-β were not statistically significant.

HS synthesis is extended with *N*-acetyl-glucosamine (GlcNAc) from the four initial monosaccharides, and the growing glycosaminoglycan chains are modified by epimerazation, deacetylation/*N*-sulfation, and *O*-sulfation (Prydz and Dalen, 2000). Thus, we used semi-quantitative RT-PCR to examine the gene expressions of enzymes involved in the biosynthesis of HS 4, 12, 24 and 48 h after FGF-2 stimulation. However, we found that gene expressions of *N*-acetylglucosaminyltransferase (GlcNAcT)-1, heparan sulfate 2-*O*-sulfotransferase (HS2ST), *N*-deacetylase/*N*-sulfotransferase (NDST)-1, NDST-2, epimerase,

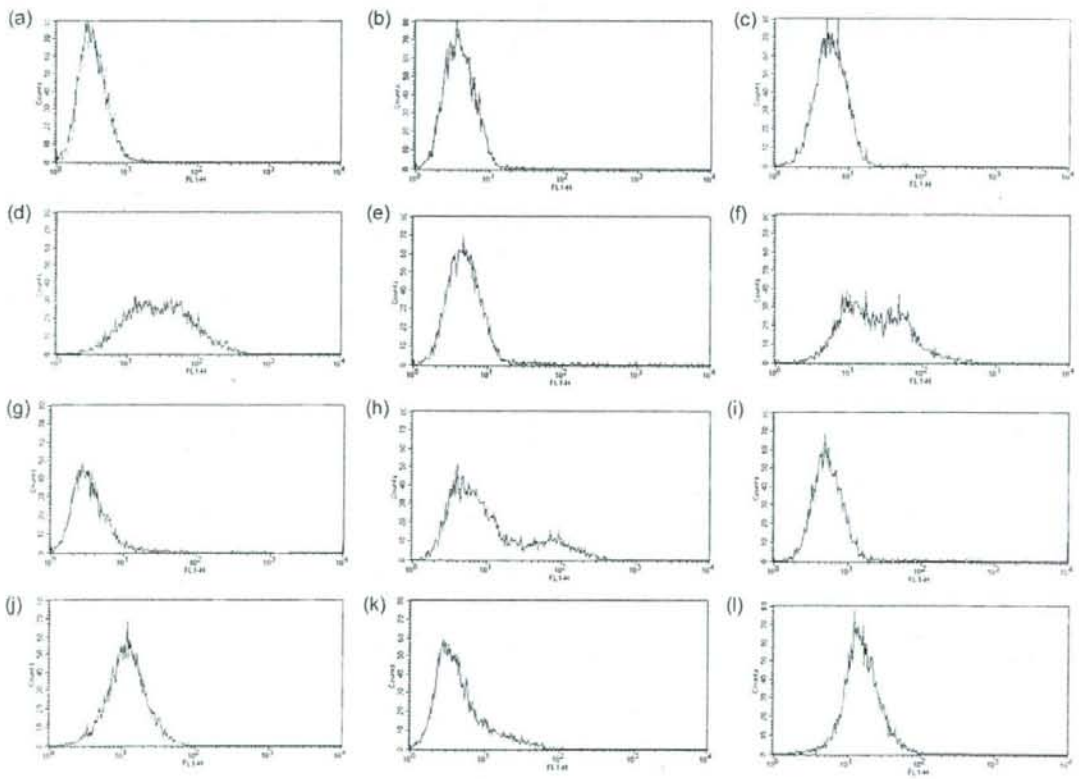

Fig. 5. FACS analysis of syndecan expression on HPDL cells. HPDL cells were incubated in 10% FCS-αMEM in the absence (gray line) or presence of FGF-2 (50 ng/ml) (black line) for 24 h (a, d, g, j), 48 h (b, e, h, k) or 72 h (c, f, i, l). At the time of the assay, cells were incubated without (a, b, c) or with the following primary antibodies: mouse anti-human syndecan-1 antibody (d, e, f); goat anti-human syndecan-2 antibody (g, h, i); mouse anti-syndecan-4 antibody (j, k, l). The cells were washed three times with PBS and incubated for 30 min at 37 °C with or without a biotinylated polyclonal anti-mouse or anti-goat antibody. After washing with PBS, staining was achieved with streptavidin-FITC.

and HPRT were not altered in FGF-2-stimulated HPDL cells at any time points examined (Fig. 3).

3.2. FGF-2 modulated syndecan expression by HPDL cells

Syndecan proteoglycan is the principal source of cell surface HS. To study the effects of FGF-2 on mRNA expression of the syndecan family in HPDL cells, RT-PCR was performed. In unstimulated HPDL cells, the mRNAs of syndecan-1 and -2 were weakly expressed and that of syndecan-4 was moderately expressed; syndecan-3 mRNA was not detected. When the HPDL cells were stimulated with FGF-2 for 24 and 48 h, the gene expression of syndecan-1, -2, and -4 was suppressed (Fig. 4).

HS proteoglycans on the cell surface are known to be shed from the cell surface into culture medium by proteolytic enzymes (Bernfield et al., 1999; Hooper et al., 1997). Next, we used FACS and immunocytochemical analyses to examine whether surface expression of HS proteoglycans on HPDL cells could be altered by FGF-2 treatment. Since syndecan-3 mRNA was not detected in either unstimulated or FGF-2-stimulated HPDL cells, we examined the expression of syndecan-1, -2, and -4 on HPDL cells. As shown in Fig. 5 FACS analysis revealed that FGF-2 lowered the expressions of syndecan-2 and -4, after 48 h and 72 h stimulation with FGF-2 and did not alter the expression of syndecan-1 on the surface of HPDL cells (Fig. 5) at any time point examined.

All three HPDL cell lines showed the decreased syndecan-2 and -4 expression in response to FGF-2 although the extent of these syndecan expression was slightly different among the cell lines. In order to confirm these alterations in HS expression on FGF-2-stimulated HPDL cells, immunocytochemical experiments were also performed. Consistent with the results of FACS experiments, expression of syndecan-2 and -4 on HPDL decreased after FGF-2 stimulation (data not shown).

Using dot blot analysis, we further examined the role of shedded syndecan in the enhanced secretion of HS in the culture supernatant of FGF-2-stimulated HPDL cells. The amounts of syndecan-1 and -2 detected in the culture supernatants of unstimulated HPDL cells were changed during the culture period. Medium from HPDL cells stimulated with FGF-2 showed no change in the amounts of syndecan-1 and -2. However, a significant increase in the amount of syndecan-4 was observed (Fig. 6). Although glypican-1, -2, -3, -6 and perlecan were also investigated, these HS proteoglycans were not detectable and no differences were observed between FGF-2-stimulated and unstimulated HPDL (data not shown).

4. Discussion

HS proteoglycan, which is composed of a core protein and HS chains, is prevalent on the cell surface and basement membrane, and has been shown to regulate various cell behaviors. It mediates signaling via interaction with matrix molecules, growth factors, or matrix metalloproteinases (MMPs). The syndecan family of four transmembrane proteoglycans is a main source of HS at cell surfaces. In this study, FGF-2 enhanced the concentration of HS in the culture medium of HPDL cells, and differentially regulated the expression of syndecan family members on the cell surface (Fig. 5). Of particular note is the fact that the level of HS in conditioned medium of FGF-2-stimulated HPDL cells was elevated in the presence of specific regulation of syndecan family members (Fig. 6). These observations suggest that individual syndecan family members may play distinct roles in response to FGF-2 (Kim et al., 1994; Lories et al., 1992).

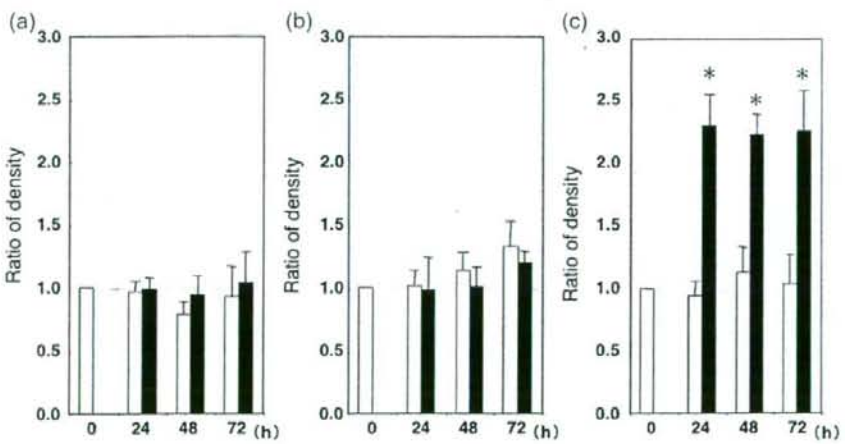

Fig. 6. Dot blot analysis of shedded syndecan in the culture supernatant of HPDL cells. Medium from FGF-2 (50 ng/ml)-stimulated (closed column) or unstimulated (open column) HPDL cells was collected after 24, 48, or 72 h. Nitrocellulose membrane was spotted with each sample, and blocked with 10% BSA to minimise non-specific binding. The membrane was incubated with HRP-conjugated rabbit anti-mouse serum for 1 h following overnight treatment with a mouse monoclonal antibody to syndecan-1 (a), -2 (b), or -4 (c). Immunoreactive bands were visualized by a chemiluminescent reaction. Data were expressed as a ratio of densitometric units relative to the value at hour 0. The experiments were performed by using three different HPDL cell lines. Mean ratios and standard deviations of the data obtained from all these cell lines are expressed in this figure ($p < 0.05$ compared to unstimulated control).

HS, a highly-sulfated glycosaminoglycan, is synthesized via multiple processes during which a series of enzymes is involved in the polymerization and modification of the HS chain. The expression of these enzymes has been reported to be regulated by several factors (Clasper et al., 1999; Moreira et al., 2003). However, FGF-2 did not activate the gene expression of the HS biosynthetic enzymes examined in this study (Fig. 3). In addition, the gene expressions of syndecan (Fig. 4) and glypican (data not shown), both of which are major HS proteoglycans on the HPDL cell surface, were not increased. These results suggest that up-regulation of the biosynthesis of HS proteoglycan does not play a major role in the elevation of the level of HS in FGF-2-stimulated HPDL cell culture medium. However, the fact that no changes in the above-mentioned genes were observed may be a timing issue. Thus, the timing may be one aspects that needs further studies.

Membrane-bound proteins such as CD43, CD44, tumor necrosis factor-α receptor, IL-6 receptor, and the syndecans are cleaved by proteolytic enzymes, sheddase or secretase, and subsequently function as soluble factors (Hooper et al., 1997). The syndecans and glypican are major cell surface proteoglycans and can be shed by proteolytic cleavage of their core proteins (David et al., 1990; Kato et al., 1998). In this study, FACS analysis revealed FGF-2-induced reduction of syndecan-2 and -4 expression on the HPDL cell surface (Fig. 5). Furthermore, dot blot analysis demonstrated an increased level of syndecan-4 in conditioned medium of FGF-2-activated HPDL cells (Fig. 6). These results suggest that FGF-2 treatment results in the loss of cell surface syndecan-4, with a concomitant increase in the level of syndecan-4 in the conditioned medium. Therefore, the current findings support the hypothesis that syndecan-4 is shed from FGF-2-activated HPDL cell surfaces. However, the mechanism of the release of each syndecan from the cell surface seems to differ with the individual syndecan family member, as the expression of each syndecan was altered differently.

Shedding of syndecan is accelerated by various factors via several intracellular signaling molecules, including extracellular signal-regulated kinase and protein kinase C, and involves the proteolytic activity responsible for cleavage of syndecan ectodomain which is regulated by MMPs and tissue inhibitors of metalloproteinases (TIMPs) (Endo et al., 2003; Fitzgerald et al., 2000; Subramanian et al., 1997). In fact, it has been reported that FGF-2 modulates the activities of some MMPs and TIMPs (Liu et al., 2002; Pintucci et al., 2003; Yasui et al., 2004). Interestingly, TIMP-3 has been reported to inhibit shedding of syndecan-1 and -4 ectodomain (Fitzgerald et al., 2000), and MMP-7 has been reported to be associated with syndecan shedding (Li et al., 2002). However, exogenous addition of these molecules to the culture medium did not affect the release of HS

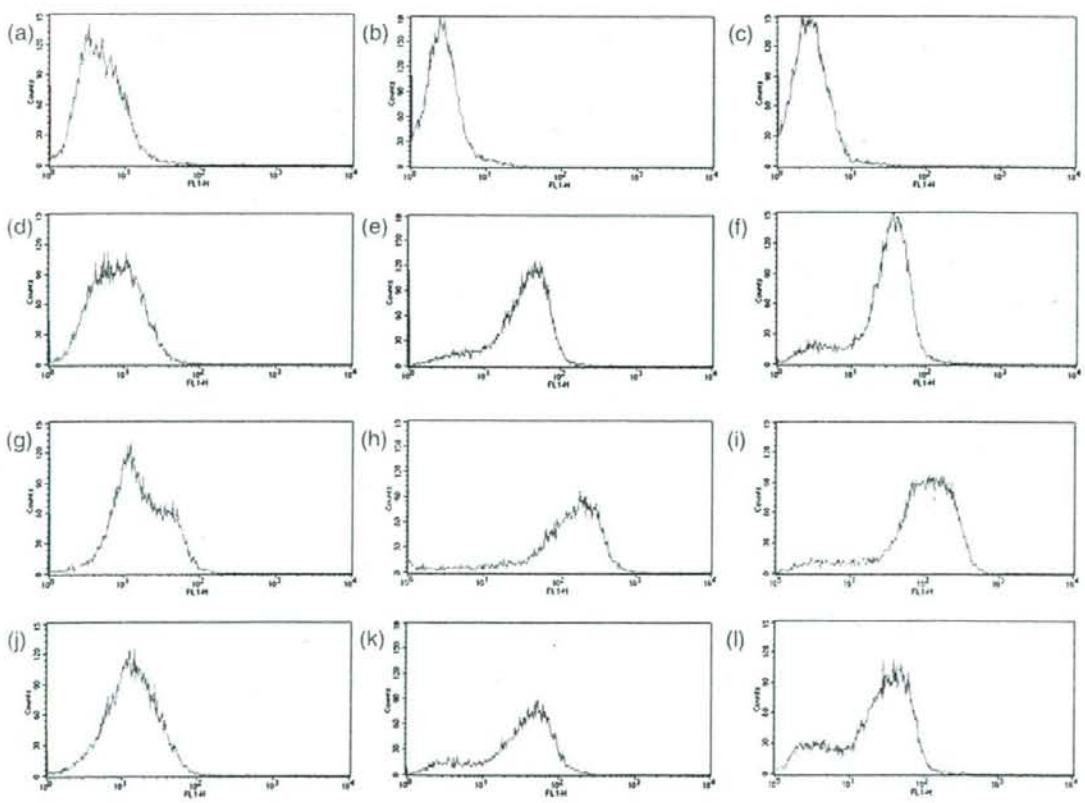

Appendix data 1.

from HPDL cells (data not shown). Further investigation is needed to clarify the mechanism by which cleavage of syndecan family members, particularly syndecan-4, occurs.

Whereas an increased level of syndecan-4 in conditioned medium of FGF-2-activated HPDL cells and a suppression of syndecan-4 expression on FGF-2-stimulated HPDL cells were observed, FGF-2 did not change the level of syndecan-2 in conditioned medium, but decreased its surface expression. HS proteoglycans on the cell surface are constitutively internalized (Yanagishita and Hascall, 1984), and FGF-2 is also internalized by both HS proteoglycan and FGF receptor (Reiland and Rapraeger, 1993; Roghani and Moscatelli, 1992). Thus, surface syndecan-2 on HPDL cells may be internalized from the cell surface following treatment of HPDL cells with FGF-2.

Glypicans are HS proteoglycans which are anchored to cell membrane via a glycosyl phosphatidyl inositol linkage. They comprise a family of six genes in mammals. Perlecan is also one of HS proteoglycan, known to be an important component of basement membrane like collagen type IV and laminin and takes part in wound healing and angiogenesis. As both HS proteoglycan are known to cleaved from cell membrane and secreted (Bernfield et al., 1999; Hacker et al., 2005), we examined their expression in the culture supernatants by dot blot analysis. However, increased expressions of glypican-1, -2, -3, -6 and perlecan were not detected in the culture supernatants of FGF-2-stimulated HPDL. Thus, it is unlikely that increase of HS in the culture supernatants of FGF-2 stimulated HPDL can be explained by shedding of those glypicans and perlecan.

It has been reported that syndecan expression was elevated at the wound edge and in lesions surrounding injured tissue, and was transiently decreased in cells migrating into the wound area (Elenius et al., 1991; Gallo et al., 1996; Iseki et al., 2002). Impaired wound healing and angiogenesis in mice lacking syndecan-4 (Echtermeyer et al., 2001), and delayed migration of corneal epithelial cells in mice lacking syndecan-1 (Stepp et al., 2002) have been observed. Over-expression of syndecan-1 and prolonged shedding is associated with delayed wound healing (Elenius et al., 2004), and reduced proliferation rate at the wound edge was also noted. Moreover, a recent study showed that cleavage of syndecan-1 was involved in cell migration (Endo et al., 2003). Also, it has been demonstrated that soluble syndecan ectodomain promotes cell growth (Yang et al., 2002), and that syndecan ectodomains accumulate in wound fluid (Subramanian et al., 1997). These findings suggest that,

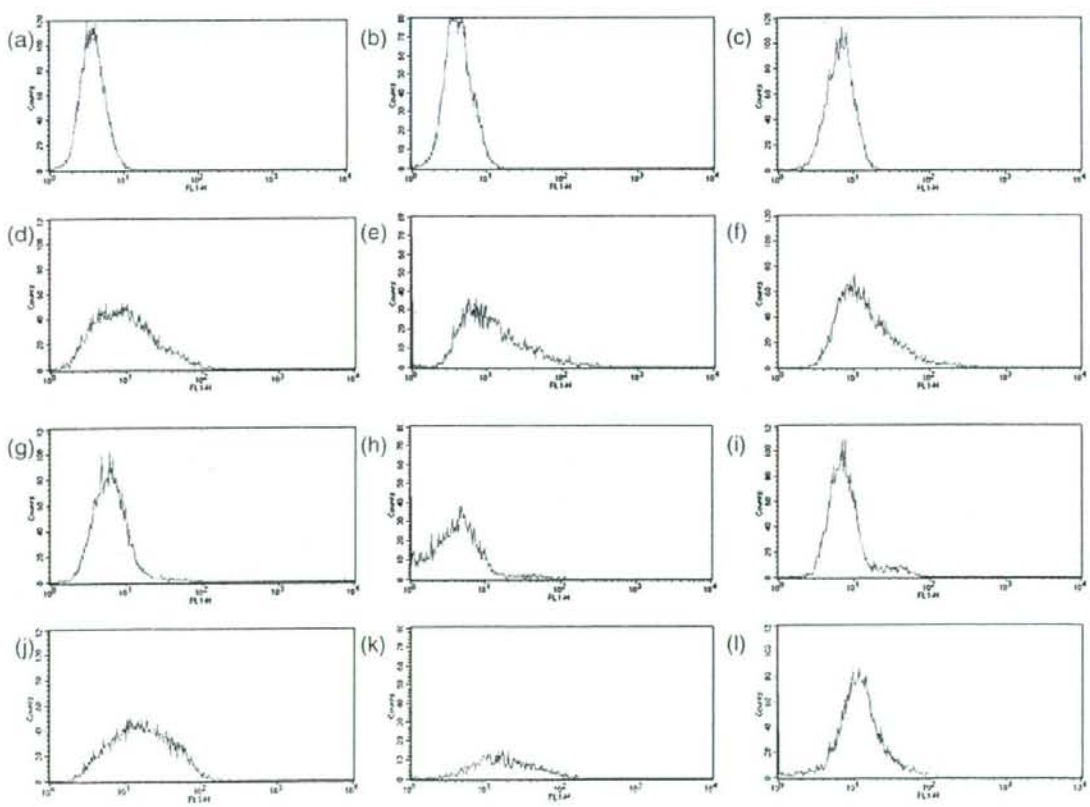

Appendix data 2.

not only the cell surface, but also the shed syndecans are closely associated with wound healing. Therefore, it is possible that FGF-2-induced shedding and accumulation of HS proteoglycan are associated with the effects of FGF-2 on acceleration of wound healing and subsequent tissue regeneration.

A close relationship between the actions of HS and FGF has also been reported (Rapraeger et al., 1991; Yayon et al., 1991). Shed proteoglycan can bind HS-binding proteins such as FGF-2 and modulate the functional effects via regulation of binding activity to receptors (Kato et al., 1998). Whether exogenous HS proteoglycans prevent or activate FGF-2 binding to FGF receptors (Bernfield et al., 1999; Kato et al., 1998; Mali et al., 1993; Modrowski et al., 2000) is dependent on the source and composition of the HS proteoglycan. Although the detailed mechanism by which shed HS or HS proteoglycan regulate FGF-2 activity remains elusive, released HS appears to modulate the interaction between FGF-2 and its receptor.

FGF-2 has been recognized to play a critical role in tissue regeneration. Indeed, it is detected at the wound (Crowley et al., 1995; Flaumenhaft et al., 1992; Murakami et al., 1999). It is postulated that in injured tissue, release of FGF-2, which is trapped to HS at the cell surface, is enhanced through proteolytic enzymes (Flaumenhaft et al., 1989). In addition, HS itself is a major constituent of tissue matrices and appears to play modulatory roles in tissue remodeling. Furthermore, we have previously reported that FGF-2 prompted regeneration of periodontal tissue that had been destroyed by the progression of periodontal diseases (Murakami et al., 1999, 2003; Takayama et al., 2001). The present observation that FGF-2 increases the level of HS in the HPDL cell culture supernatant suggests positive or negative feedback regulation during wound healing and regeneration processes in damaged periodontal tissues.

Acknowledgements

This work was supported by Grants-in-Aid for Scientific Research (the Japan Society for the Promotion of Science Nos. 17390560, 17209065 and 17390561, 18659622, 18791591, 18890107) and the 21st Century COE entitled, "Origination of Frontier BioDentistry", Osaka University Graduate School of Dentistry supported by the Ministry of Education, Culture, Sports, Science and Technology. We thank Kaken Pharmaceutical Co. Ltd. and Seikagaku Co. for providing technical assistance, valuable reagents and advice.

Appendix A

Appendix data 1 and 2 FACS analysis of syndecan expression on HPDL cells. HPDL cells (the other cells than that in Fig. 5) were incubated in 10% FCS-αMEM in the absence (gray line) or presence of FGF-2 (50 ng/ml) (black line) for 24 h (a, d, g, j), 48 h (b, e, h, k) or 72 h (c, f, i, l). At the time of the assay, cells were incubated without (a, b, c) or with the following primary antibodies: mouse anti-human syndecan-1 antibody (d, e, f); goat anti-human syndecan-2 antibody (g, h, i); mouse anti-syndecan-4 antibody (j, k, l). The cells were washed three times with PBS and incubated for 30 min at 37 °C with or without a biotinylated polyclonal anti-mouse or anti-goat antibody. After washing with PBS, staining was achieved with streptavidin-FITC.

References

Bernfield, M., Gotte, M., Park, P.W., Reizes, O., Fitzgerald, M.L., Lincecum, J., Zako, M., 1999. Functions of cell surface heparan sulfate proteoglycans. Annu. Rev. Biochem. Allied Res. India 68, 729–777.

Bikfalvi, A., Klein, S., Pintucci, G., Rifkin, D.B., 1997. Biological roles of fibroblast growth factor-2. Endocr. Rev. 18, 26–45.

Clasper, S., Vekemans, S., Fiore, M., Plebanski, M., Wordsworth, P., David, G., Jackson, D.G., 1999. Inducible expression of the cell surface heparan sulfate proteoglycan syndecan-2 (fibroglycan) on human activated macrophages can regulate fibroblast growth factor action. J. Biol. Chem. 274, 24113–24123.

Crowley, S.T., Ray, C.J., Nawaz, D., Majack, R.A., Horwitz, L.D., 1995. Multiple growth factors are released from mechanically injured vascular smooth muscle cells. Am. J. Physiol. 269, H1641–H1647.

David, G., Lories, V., Decock, B., Marynen, P., Cassiman, J.J., Van den Berghe, H., 1990. Molecular cloning of a phosphatidylinositol-anchored membrane heparan sulfate proteoglycan from human lung fibroblasts. J. Cell Biol. 111, 3165–3176.

Echtermeyer, F., Streit, M., Wilcox-Adelman, S., Saoncella, S., Denhez, F., Detmar, M., Goetinck, P., 2001. Delayed wound repair and impaired angiogenesis in mice lacking syndecan-4. J. Clin. Invest. 107, R9–R14.

Elenius, K., Vainio, S., Laato, M., Salmivirta, M., Thesleff, I., Jalkanen, M., 1991. Induced expression of syndecan in healing wounds. J. Cell Biol. 114, 585–595.

Elenius, K., Paul, S., Allison, G., Sun, J., Klagsbrun, M., 1997. Activation of HER4 by heparin-binding EGF-like growth factor stimulates chemotaxis but not proliferation. EMBO J. 16, 1268–1278.

Elenius, V., Gotte, M., Reizes, O., Elenius, K., Bernfield, M., 2004. Inhibition by the soluble syndecan-1 ectodomains delays wound repair in mice overexpressing syndecan-1. J. Biol. Chem. 279, 41928–41935.

Endo, K., Takino, T., Miyamori, H., Kinsen, H., Yoshizaki, T., Furukawa, M., Sato, H., 2003. Cleavage of syndecan-1 by membrane type matrix metalloproteinase-1 stimulates cell migration. J. Biol. Chem. 278, 40764–40770.

Fitzgerald, M.L., Wang, Z., Park, P.W., Murphy, G., Bernfield, M., 2000. Shedding of syndecan-1 and -4 ectodomains is regulated by multiple signaling pathways and mediated by a TIMP-3-sensitive metalloproteinase. J. Cell Biol. 148, 811–824.

Flaumenhaft, R., Moscatelli, D., Saksela, O., Rifkin, D.B., 1989. Role of extracellular matrix in the action of basic fibroblast growth factor: matrix as a source of growth factor for long-term stimulation of plasminogen activator production and DNA synthesis. J. Cell. Physiol. 140, 75–81.

Flaumenhaft, R., Abe, M., Mignatti, P., Rifkin, D.B., 1992. Basic fibroblast growth factor-induced activation of latent transforming growth factor beta in endothelial cells: regulation of plasminogen activator activity. J. Cell Biol. 118, 901–909.

Gallo, R., Kim, C., Kokenyesi, R., Adzick, N.S., Bernfield, M., 1996. Syndecans-1 and -4 are induced during wound repair of neonatal but not fetal skin. J. Invest. Dermatol. 107, 676–683.

Hacker, U., Nybakken, K., Perrimon, N., 2005. Heparan sulphate proteoglycans: the sweet side of development. Nat. Rev., Mol. Cell Biol. 6, 530–541.

Hooper, N.M., Karran, E.H., Turner, A.J., 1997. Membrane protein secretases. Biochem. J. 321, 265–279.

Iseki, K., Hagino, S., Mori, T., Zhang, Y., Yokoya, S., Takaki, H., Tase, C., Murakawa, M., Wanaka, A., 2002. Increased syndecan expression by pleiotrophin and FGF receptor-expressing astrocytes in injured brain tissue. Glia 39, 1–9.

Ishiguro, K., Kadomatsu, K., Kojima, T., Muramatsu, H., Nakamura, E., Ito, M., Nagasaka, T., Kobayashi, H., Kusugami, K., Saito, H., Muramatsu, T., 2000. Syndecan-4 deficiency impairs the fetal vessels in the placental labyrinth. Dev. Dyn. 219, 539–544.

Kainulainen, V., Wang, H., Schick, C., Bernfield, M., 1998. Syndecans, heparan sulfate proteoglycans, maintain the proteolytic balance of acute wound fluids. J. Biol. Chem. 273, 11563–11569.

Kato, M., Wang, H., Kainulainen, V., Fitzgerald, M.L., Ledbetter, S., Ornitz, D.M., Bernfield, M., 1998. Physiological degradation converts the soluble syndecan-

1 ectodomain from an inhibitor to a potent activator of FGF-2. Nat. Med. 4, 691–697.

Kim, C.W., Goldberger, O.A., Gallo, R.L., Bernfield, M., 1994. Members of the syndecan family of heparan sulfate proteoglycans are expressed in distinct cell-, tissue-, and development-specific patterns. Mol. Biol. Cell 5, 797–805.

Li, Q., Park, P.W., Wilson, C.L., Parks, W.C., 2002. Matrilysin shedding of syndecan-1 regulates chemokine mobilization and transepithelial efflux of neutrophils in acute lung injury. Cell 111, 635–646.

Liu, J.F., Crepin, M., Liu, J.M., Barritault, D., Ledoux, D., 2002. FGF-2 and TPA induce matrix metalloproteinase-9 secretion in MCF-7 cells through PKC activation of the Ras/ERK pathway. Biochem. Biophys. Res. Commun. 293, 1174–1182.

Lories, V., Cassiman, J.J., Van den Berghe, H., David, G., 1992. Differential expression of cell surface heparan sulfate proteoglycans in human mammary epithelial cells and lung fibroblasts. J. Biol. Chem. 267, 1116–1122.

Mali, M., Elenius, K., Miettinen, H.M., Jalkanen, M., 1993. Inhibition of basic fibroblast growth factor-induced growth promotion by overexpression of syndecan-1. J. Biol. Chem. 268, 24215–24222.

Modrowski, D., Basle, M., Lomri, A., Marie, P.J., 2000. Syndecan-2 is involved in the mitogenic activity and signaling of granulocyte-macrophage colony-stimulating factor in osteoblasts. J. Biol. Chem. 275, 9178–9185.

Moreira, C.R., Porcionatto, M.A., Dietrich, C.P., Nader, H.B., 2003. Effect of bradykinin and PMA on the synthesis of proteoglycans during the cell cycle of endothelial cells in culture. Int. J. Immunopharmacol. 3, 293–298.

Murakami, S., Takayama, S., Ikezawa, K., Shimabukuro, Y., Kitamura, M., Nozaki, T., Terashima, A., Asano, T., Okada, H., 1999. Regeneration of periodontal tissues by basic fibroblast growth factor. J. Periodontal Res. 34, 425–430.

Murakami, S., Takayama, S., Kitamura, M., Shimabukuro, Y., Yanagi, K., Ikezawa, K., Saho, T., Nozaki, T., Okada, H., 2003. Recombinant human basic fibroblast growth factor (bFGF) stimulates periodontal regeneration in class II furcation defects created in beagle dogs. J. Periodontal Res. 38, 97–103.

Nugent, M.A., Iozzo, R.V., 2000. Fibroblast growth factor-2. Int. J. Biochem. Cell Biol. 32, 115–120.

Park, P.W., Pier, G.B., Preston, M.J., Goldberger, O., Fitzgerald, M.L., Bernfield, M., 2000. Syndecan-1 shedding is enhanced by LasA, a secreted virulence factor of *Pseudomonas aeruginosa*. J. Biol. Chem. 275, 3057–3064.

Potenza, G., Yu, P.J., Sharony, R., Baumann, F.G., Saponara, F., Frasca, A., Galloway, A.C., Moscatelli, D., Mignatti, P., 2003. Induction of stromelysin-1 (MMP-3) by fibroblast growth factor-2 (FGF-2) in FGF-2 microvascular endothelial cells requires prolonged activation of extracellular signal-regulated kinases-1 and -2 (ERK-1/2). J. Cell. Biochem. 90, 1015–1025.

Prydz, K., Dalen, K.T., 2000. Synthesis and sorting of proteoglycans. J. Cell Sci. 113, 193–205.

Rapraeger, A.C., Krufka, A., Olwin, B.B., 1991. Requirement of heparan sulfate for bFGF-mediated fibroblast growth and myoblast differentiation. Science 252, 1705–1708.

Reiland, J., Rapraeger, A.C., 1993. Heparan sulfate proteoglycan and FGF receptor target basic FGF to different intracellular destinations. J. Cell Sci. 105, 1085–1093.

Roghani, M., Moscatelli, D., 1992. Basic fibroblast growth factor is internalized through both receptor-mediated and heparan sulfate-mediated mechanisms. J. Biol. Chem. 267, 22156–22162.

Shimabukuro, Y., Ichikawa, T., Takayama, S., Yamada, S., Takedachi, M., Terakura, M., Hashikawa, T., Murakami, S., 2005. Fibroblast growth factor-2 regulates the synthesis of hyaluronan by human periodontal ligament cells. J. Cell. Physiol. 203, 557–563.

Somerman, M.J., Archer, S.Y., Imm, G.R., Foster, R.A., 1988. A comparative study of human periodontal ligament cells and gingival fibroblasts in vitro. J. Dent. Res. 67, 66–70.

Stepp, M.A., Gibson, H.E., Gala, P.H., Iglesia, D.D., Pajoohesh-Ganji, A., Pal-Ghosh, S., Brown, M., Aquino, C., Schwartz, A.M., Goldberger, O., Hinkes, M.T., Bernfield, M., 2002. Defects in keratinocyte activation during wound healing in the syndecan-1-deficient mouse. J. Cell Sci. 115, 4517–4531.

Subramanian, S.V., Fitzgerald, M.L., Bernfield, M., 1997. Regulated shedding of syndecan-1 and -4 ectodomains by thrombin and growth factor receptor activation. J. Biol. Chem. 272, 14713–14720.

Takayama, S., Murakami, S., Shimabukuro, Y., Kitamura, M., Okada, H., 2001. Periodontal regeneration by FGF-2 (bFGF) in primate models. J. Dent. Res. 80, 2075–2079.

Yanagishita, M., Hascall, V.C., 1984. Metabolism of proteoglycans in rat ovarian granulosa cell culture. Multiple intracellular degradative pathways and the effect of chloroquine. J. Biol. Chem. 259, 10270–10283.

Yang, Y., Yaccoby, S., Liu, W., Langford, J.K., Pumphrey, C.Y., Theus, A., Epstein, J., Sanderson, R.D., 2002. Soluble syndecan-1 promotes growth of myeloma tumors in vivo. Blood 100, 610–617.

Yasui, H., Andoh, A., Bamba, S., Inatomi, O., Ishida, H., Fujiyama, Y., 2004. Role of fibroblast growth factor-2 in the expression of matrix metalloproteinases and tissue inhibitors of metalloproteinases in human intestinal myofibroblasts. Digestion 69, 34–44.

Yayon, A., Klagsbrun, M., Esko, J.D., Leder, P., Ornitz, D.M., 1991. Cell surface, heparin-like molecules are required for binding of basic fibroblast growth factor to its high affinity receptor. Cell 64, 841–848.

Journal of Cellular Physiology

Fibroblast Growth Factor-2 Regulates Expression of Osteopontin in Periodontal Ligament Cells

YOSHIMITSU TERASHIMA, YOSHIO SHIMABUKURO, HIROAKI TERASHIMA, MASAO OZASA, MAMI TERAKURA, KAZUHIKO IKEZAWA, TOMOKO HASHIKAWA, MASAHIDE TAKEDACHI, HIROYUKI OOHARA, SATORU YAMADA, AND SHINYA MURAKAMI*

Department of Periodontology, Division of Oral Biology and Disease Control, Osaka University Graduate School of Dentistry, Osaka, Japan

Osteopontin is a protein found in the bone-related matrix and plays multiple regulatory roles in mineralizing and non-mineralizing tissue. In osteogenic cell-lines, the expression of osteopontin increases with the progression of differentiation, but both the expression and function of osteopontin vary with the cell type and its activation state. In this study, we examined the expression of osteopontin by clones established from mouse periodontal ligament, in response to inorganic phosphate and fibroblast growth factor (FGF)-2, which can induce periodontal tissue regeneration. The involvement of inorganic phosphate in the expression of osteopontin during the course of cell differentiation of a clone MPDL22 was confirmed by addition of foscarnet, an inorganic phosphate transport inhibitor. Although FGF-2 decreased the mRNA expression of almost every bone-related protein in MPDL22, FGF-2 upregulated the expression of osteopontin in MPDL22 at both mRNA and protein levels. Interestingly, FGF-2 enhanced the concentration of osteopontin in the culture supernatant of MPDL22, whereas inorganic phosphate did not. The FGF-2-induced osteopontin in the culture supernatant seems to be involved in cell survival activity. An immunohistochemical study showed that the FGF-2-induced osteopontin was mainly present in perinuclear matrices while the inorganic phosphate-induced osteopontin was associated with extracellular matrices in addition to perinuclear matrices. The present results indicated that FGF-2 induces unique expression of osteopontin, which may play a role different from the other bone-related proteins during the process of periodontal tissue regeneration by FGF-2.

J. Cell. Physiol. 216: 640–650, 2008

Osteopontin is a non-collagenous phosphoprotein found in bone extracellular matrix and is known as an osteogenesis marker. However, several lines of reports have revealed that its roles for the regulation of matrix mineralization and bone cell function is controversial although the detailed mechanism regulating the bioactivity of osteopontin in calcified tissues has not been fully elucidated. In addition to those functions as a calcified tissue-related molecule, broad biological functions of osteopontin have also been demonstrated in association with tumor biology (Senger et al., 1983), tissue injury and repair (Giachelli et al., 1994; Liaw et al., 1998), dystrophic calcification (Srivatsa et al., 1997), and inflammation (Patarca et al., 1989; Nau et al., 1997). In fact, osteopontin is synthesized by a variety of cell types, such as epithelial cells, endothelial cells, smooth muscle cells, fibroblasts, immune cells like T cells, NK cells, macrophages in addition to osteoblasts and osteoclasts (O'Regan and Berman, 2000; Denhardt et al., 2001b).

Periodontal tissue, which is a tooth-supporting apparatus, consists of gingiva, alveolar bone, cementum and periodontal ligament (PDL). PDL plays an important role as a reservoir of mesenchymal stem cells (Seo et al., 2004). Thus, the cells in PDL tissue are critical participants during the tissue remodeling and regeneration process when breakdown of periodontal tissue caused by bacterial biofilm or mechanical stress is healed. We found that topical application of fibroblast growth factor (FGF)-2 to experimentally created alveolar bone defects prompted significant periodontal tissue regeneration accompanying the formation of new bone and cementum (Murakami et al., 1999, 2003; Takayama et al., 2001). In vitro studies revealed that FGF-2 can promote strong growth of PDL cells, and regulate the production of extracellular matrix, which play important roles for desirable periodontal tissue regeneration (Takayama et al., 1997; Shimabukuro et al., 2005). Interestingly, we recently found that FGF-2 suppressed the expression of bone-related proteins, such as type I collagen, osteocalcin and bone sialoprotein, but prompted the expression of osteopontin by PDL cells.

In this study, utilizing PDL clones obtained from mouse PDL (MPDL) tissues (Yamada et al., 2007), we investigated the expression of osteopontin by PDL cells in detail. In particular, we focused on FGF-2-dependent expression of osteopontin in comparison with inorganic phosphate, which facilitates osteogenic differentiation, and examined its possible biological roles.

Materials and Methods

Materials

Tissue culture supplies and plastic Leighton tubes were obtained from Corning Coster (New York, NY). Alpha Modification of

Contract grant sponsor: Japan Society for the Promotion of Science;
Contract grant numbers: Grants-in-aid 16209056, 17209065, 17390560, 16209063, 17390561, 18890107.
Contract grant sponsor: Ministry of Education, Culture, Sports, Science and Technology.

*Correspondence to: Shinya Murakami, Department of Periodontology, Division of Oral Biology and Disease Control, Osaka University Graduate School of Dentistry, 1-8 Yamadaoka, Suita, Osaka 565-0871, Japan. E-mail: ipshinya@dent.osaka-u.ac.jp

Received 14 June 2007; Accepted 8 February 2008

DOI: 10.1002/jcp.21443

Eagles Medium (α-MEM) was a product of ICN Biomedicals, Inc. (Costa Mesa, CA). Bovine calf serum (FCS) was purchased from JRH Biosciences (Lenexa, KS). Bovine serum albumin and β-glycerophosphate (BGP) and bisbenzimidazole (Hoechest 33258) were products of Sigma (St. Louis, MO). Human recombinant FGF-2 was obtained from Kaken Pharmaceutical Co., Ltd. (Tokyo, Japan). Goat anti-mouse osteopontin antibody and goat anti-β-actin antibody was obtained from R & D Systems, Inc. (Minneapolis, MN).

Isolation of mouse periodontal cell clones

MPDL cell clones were isolated as previously described (Yamada et al., 2007). Cell cloning was done twice using the limiting dilution method in α-MEM supplemented with 10% FCS and 100 ng/ml FGF-2. Twenty-nine MPDL clonal cell lines were obtained and classified by alkaline phosphatase (ALPase) activity. We selected two of these clones: one clone, MPDL22 was characterized by a high level of alkaline phosphatase (ALPase) and the other clone, MPDL6 exhibit low level in ALPase even in the presence of BGP and ascorbic acid. MPDL22 cells were positive for collagen type I, Runx2, Msx2, Dlx5, and Osterix mRNA (Yamada et al., 2007).

Assay of ALPase activity

ALPase activity was investigated according to the procedure of Bessey and Lowry (1946). The PDL clones were seeded in 24-well culture dishes (1×10^5 cells/well) with standard medium containing 50 μg/ml ascorbic acid and 10 mM BGP. They were cultured for indicated days in this medium, which was changed every 2 days. After washed twice with saline, the cells were homogenized in a glass homogenizer in 1 ml of 0.9% NaCl, 0.2% Triton X-100 at 0–4°C and centrifuged for 15 min at 12,000g. ALPase activity in the supernatant was determined using *p*-nitrophenyl phosphate (*p*NP) as substrate. The supernatant was assayed in a 0.5 M Tris/HCl buffer (pH 9.0) containing 0.5 mM *p*NP and 0.5 mM $MgCl_2$. The reaction mixture was incubated at 37°C for 30 min, and the reaction was stopped by addition of 0.25 volume of 1 N NaOH. Hydrolysis of *p*NP was monitored as change in A_{410} with a spectrometer (Hitachi Instruments Service Co., Ltd., Tokyo, Japan). *p*-Nitrophenol was used as a standard. One unit of activity was defined as the amount hydrolyzing 1 nmol of *p*-NP in 30 min.

Cellular DNA content

DNA content was measured by a modification of the method of Labarca and Paigen (1980). The PDL clones were seeded in 24-well culture dishes (1×10^5 cells/well) with standard medium containing 50 μg/ml ascorbic acid and 10 mM BGP. They were cultured for 20 days in this medium, which was changed every 2 day. Alteration of DNA content of the cells was determined as follows. The PDL clones were washed with PBS and then homogenized at 0–4°C in 1 ml of 2 M NaCl/25 mM Tris–HCl (pH 7.4). After centrifugation at 12,000g for 10 min, 25 μl of 5 μg/ml bisbenzimidazole was added to 100 μl of the supernatant. The fluorescent spectra at emission 458 nm after excitation at 356 nm was monitored by a spectrophotometer. The concentration of DNA in the samples was determined by a standard curve made at various concentrations of calf thymus DNA.

Alizarin red staining

Histochemical staining of calcium was performed by modification of the alizarin red staining method (Dahl, 1952). The cell layers were washed twice with saline and then fixed with dehydrated ethanol. After fixation, the cell layers were stained with 1% alizarin red S in 0.1% NH_4OH (pH 6.5) for 5 min, then washed with H_2O.

Detection of osteopontin mRNA by RT-PCR

MPDL clones were seeded at a density of 1×10^6 cells/dish in a 60 mm dish and grown to confluence in standard medium. Following 24 h activation of MPDL with or without FGF-2 (100 ng/ml), total RNA was isolated from each cell by RNAzol™ (Cinna/Biotecx Laboratories, Inc., Friendswood, TX) according to the manufacturer's instructions. The precipitated RNA was resolved in 0.1% diethylpyrocarbonate-treated distilled water (DEPC-treated H_2O). cDNA synthesis and amplification via PCR were performed according to the methods described by Takayama et al. (1997). For PCR analysis, we incubated a 40 ml cDNA synthesis reaction mixture per RNA sample at 37°C for 60 min. Each 40 μl cDNA synthesis reaction mixture contained: 5.2 μl of DEPC-treated H_2O; 4 μl 10× PCR buffer II (100 mM Tris–HCl pH 8.3, 500 mM KCl; Perkin Elmer Cetus, Norwalk, CT); 6 μl 25 mM $MgCl_2$; 4 μl of each 10 mM deoxynucleotide-triphosphate (Takara Shuzo Co. Ltd., Kyoto, Japan); 0.4 μl 20 U/ml RNase inhibitor (Perkin Elmer Cetus); 1 ml 50 U/ml M-MLV reverse transcriptase; 4 μl 0.25 μg/ml RNA sample. After incubation, all samples were heated to 94°C for 5 min to inactivate the reverse transcriptase.

Oligonucleotide PCR primers specific for type I collagen, Pebp2αA/Cbfa1, Osf-2/Til-1/Cbfa1, bone sialo protein, osteonectin, osteopontin, osteocalcin, and β-actin mRNA were synthesized by Clontech Laboratories, Inc. (Palo Alto, CA) (Table 1). The cDNA samples prepared above were amplified by adding to a PCR reaction mixture which included 10 mM Tris–HCl buffer (pH 8.3), 1.5 mM $MgCl_2$, 50 mM KCl, 0.15 mM dNTP mixture, 1.25 U AmpliTaq Gold™ (Perkin Elmer), and 0.2 μM sense and antisense oligonucleotide primers. The PCR reaction mixture was overlaid with mineral oil (Aldrich Chemical Company,

TABLE 1. Primers utilized for reverse transcription-polymerase chain reaction

Primers	Size (bp)	Sequence
Type I collagen	268	Sense 5′-TCTCCACTCTTCTAGTTCCT-3′ Antisense 5′-TTGGGTCATTTCCACATGC-3′
Pebp2αA/Cbfa1	303	Sense 5′-AGGATTTTATCATGGACACG-3′ Antisense 5′-TCTTTCCTGTGCGATAGAGT-3′
Osf-2/Til-1/Cbfa1	386	Sense 5′-GAGGGCACAAGTTCTATCTGGA-3′ Antisense 5′-GGTGGTCCGCGATGATCTC-3′
Bone sialo protein	430	Sense 5′-ACCGGCCACGCTACTTTCTTT-3′ Antisense 5′-GACCGCCAGCTCGTTTTCA-3′
Osteonectin	453	Sense 5′-CGCCCCCTGCCTGGATTCCG-3′ Antisense 5′-GATCACCAGATCCTTGTTGATGTCCTGC-3′
Osteopontin	485	Sense 5′-CTGCTAGTACACAAGCAGACA-3′ Antisense 5′-CATGAGAAATTCGGAATTTCAG-3′
Osteocalcin	264	Sense 5′-CTGGCCCTGGCTGCGCTCTGT-3′ Antisense 5′-GGTCCTAAATAGTGATACCGTAGATGCG-3′
β-actin	388	Sense 5′-AGCAAGAGAGGTATCCT-3′ Antisense 5′-ATGAGGTAGTCTGTCAGGT-3′

Inc., Milwaukee, WI) and subjected to amplification for two or three different number of cycles using a DNA Thermal cycler 480 (Perkin Elmer). After initial denaturation at 94°C for 4 min, each cycle consisted of 94°C for 45 sec, 60°C for 45 sec, and 72°C for 2 min. PCR products were analyzed by electrophoresis at 100 V for 30 min on 1.5% TAE agarose gel (NIPPON GENE Co., Ltd., Toyama, Japan) containing 0.5 μg/ml ethidium bromide.

Protein extraction from plasma membrane

Cells (1×10^8) were collected in PBS by scraping cells and washed with ice cold PBS. Resuspended cells were homogenized on ice for 30–50 times and centrifuged at 700*g* for 10 min at 4°C, and then the supernatant was collected and centrifuged at 10,000*g* for 30 min at 4°C. The supernatant was used as the cytosol fraction. The pellet was resuspended, centrifuged at 1,000*g* for 5 min and used as plasma membrane protein.

Western blotting analysis

MPDL clones which had been grown to subconfluence in standard medium, were cultured without FCS for 48 h, and then incubated in the presence or absence of FGF-2 or inorganic phosphate. At the end of the culture, cells were harvested in lysis buffer (150 mM NaCl, 1% Triton-X-100, 1 mM EGTA, 1.5 mM $MgCl_2$, 10 mM sodium pyrophosphate, 10 mg of aprotinin/ml, and 10 mg of leupeptin/ml) and centrifuged at 10,000*g*. Protein was resolved on SDS–PAGE and transferred onto nitrocellulose membrane. Filters were incubated with 10% bovine serum albumin for 1 h and subsequently with goat anti-osteopontin antibody (R & D Systems, Inc.) or mouse monoclonal anti-β-actin antibody (mouse IgG 1 isotype) (Sigma) for 3 h at room temperature. Immune complex were detected using an enhanced chemiluminence kit (ECL, Amersham, Little Chalfont, England).

Histochemical analysis

MPDL clones were cultured onto a coverglass (Matsunami Co., Osaka, Japan) mounted on a 35-mm plate. Cells were fixed for 10 min in 2% paraformaldehyde and either treated with PBS including with 0.1% Triton X to permeabilize cell membrane or not. After fixation, the cell monolayer was washed in PBS, incubated with goat anti-osteopontin antibody, rabbit anti-type I collagen antibody (R & D Systems, Inc.), rabbit anti-fibronectin antibody (Chemicon International, Temecula, CA) at 50 μg/ml in PBS for 5 h or overnight at room temperature, and then washed in PBS three times, 30 min each time. Then, cells were incubated with Alexa Fluor 488 conjugated donkey anti-goat antibody (Molecular Probes, Engene, OK) or Alexa Fluor 546 goat anti-rabbit IgG. Immunofluorescence was measured by confocal laser scanning microscopy (Olympus Co., Tokyo, Japan). Reagent controls consisted of cell monolayer processed as above but incubated with PBS.

Determination of osteopontin in culture supernatants

MPDL clones were placed in a 24 well plate (Corning Coster) at 1×10^4 cells in complete media. Following serum starvation for 48 h, MPDL clones were stimulated with or without FGF-2 (100 ng/ml) or inorganic phosphate (10 mM). At the end of the incubation period, the supernatants were collected and stored at −20°C until determination of osteopontin level. The osteopontin levels in culture supernatants were measured by using an enzyme-linked immunosorbent assay (ELISA) kit (Immuno-Biological Laboratories Co., Ltd., Gunma, Japan) according to the manufacturer's instructions.

Cell survival assay

Apoptosis was detected using a cell death detection ELISA^{plus} kit following the instruction manual. MPDL22 was treated with 2 ng/ml of camptothecin for 6 h at 37°C to induce apoptosis and centrifuged (200*g*). The cells were lysed with lysis buffer and the lysate was centrifuged (200*g*) for 10 min. A 20 μl aliquot from the supernatant was transferred into the streptoavidin-coated 96-well plate. Anti-histone-biotin and anti-DNA-peroxidase were added to each well, incubated for 2 h at room temperature, and then rinsed with incubation buffer. Color was developed with ABTS solution and absorbance was measured at 405 nm using a microplate reader (Model 550, Bio-Rad Laboratory, Hercules, CA). Quantitative determination of the amount of nucleosomes was calculated from the standard.

Results

MPDL22 exhibited expression of osteopontin

We established 29 clones from MPDL tissues. They were composed of heterogenous phenotypes in terms of ALPase activity. One clone, MPDL22, showed cell differentiation in the presence of ascorbic acid and BGP and formed mineralized nodules in the presence of a high level of ALPase in vitro (Fig. 1). Another clone, MPDL6, showed impaired differentiation ability in the presence of a low level of alkaline phosphatase. Using these clones, we investigated the expression of osteopontin, as an early differentiation marker of osteoblasts. Western blot analysis indicated that expression of osteopontin was elevated with a peak expression on day 14 and decreased afterward when MPDL22 was cultured in the presence of ascorbic acid and BGP (Fig. 2a). Consistent with the results of western blot analysis, immunohistochemical analysis revealed the increased expression of osteopontin by MPDL22 at day 12 (Fig. 2b). Compared with MPDL22, MPDL6 exhibited only a marginal increase of expression of osteopontin in both western blot and immunohistochemical analysis (Fig. 2a,b). β-actin expression which was used as an internal control did not altered between MPDL22 and MPDL6.

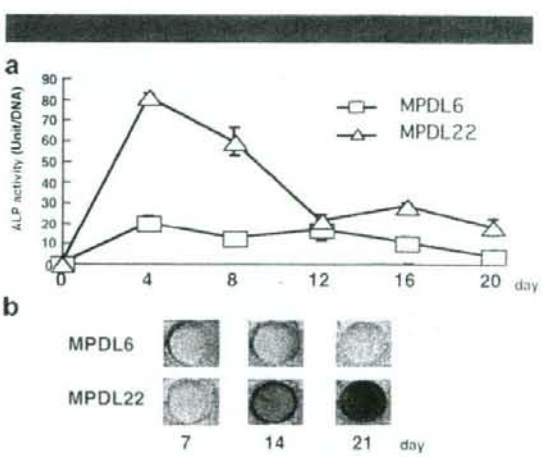

Fig. 1. Kinetics of ALPase activity and mineral deposition by MPDL6 and MPDL22 during cell differentiation. MPDL6 or MPDL22 was cultured in the presence of ascorbic acid (50 μg/ml) and BGP (10 mM) for indicated days. a: Cells were homogenized and centrifuged. ALPase activity in the supernatant was measured using *p*NP. Hydrolysis of *p*NP was monitored as a change in A_{410} with a spectrometer. b: Cell monolayers were fixed with dehydrated ethanol and stained with 1% alizarin red S in 0.1% NH_4OH for 5 min. Results of one representative experiment out of three separate experiments are shown. [Color figure can be viewed in the online issue, which is available at www.interscience.wiley.com.]

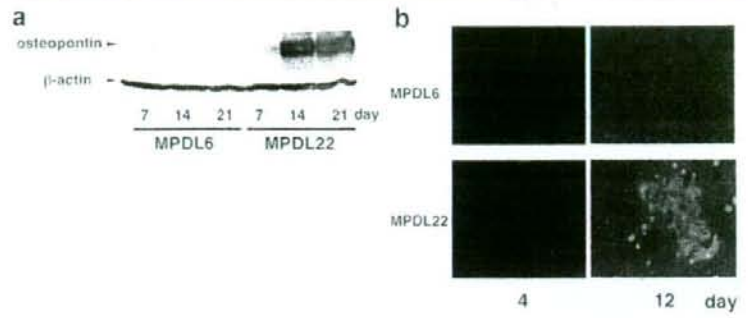

Fig. 2. Expression of osteopontin by MPDL6 and MPDL22 during cell differentiation. a: MPDL6 and MPDL22 were cultured in the presence of 50 μg/ml ascorbic acid and 10 mM BGP for 7, 14, or 21 days. Samples were electrophoresed on 8% mini-gels, transblotted onto nitrocellulose membrane. Immunoreactive osteopontin was detected using a primary goat anti-osteopontin polyclonal antibody and chemiluminece kit. Immunoreactive β-actin was also detected as an internal control. b: MPDL6 and MPDL22 were cultured in the presence of 50 μg/ml ascorbic acid and 10 mM BGP for 4 or 12 days. Cell monolayers were fixed with 2% paraformaldehyde and incubated with or without goat anti-osteopontin polyclonal antibody after incubation with Alexa Fluor 488 conjugated anti-goat IgG antibody. Results of one representative experiment out of three separate experiments are shown.

Inorganic phosphate contributes to mineralization of MPDL22 and prompts its expression of osteopontin

During in vitro differentiation of osteoblasts, levels of ALPase activity and extracellular inorganic phosphate are increased (Bellows et al., 1992; Chung et al., 1992). Recently, inorganic phosphate has been found to regulate the in vitro differentiation of osteoblasts with elevation of bone-related gene and mineralization through a inorganic phosphate transport system as a signaling molecule (Beck et al., 2003). The action of inorganic phosphate during the differentiation of PDL cells was confirmed by directly examining the effects of inorganic phosphate on mineralization by MPDL22. Inorganic phosphate elicited mineralized nodule formation by MPDL22 at day 7 as in the long-term culture with ascorbic acid and BGP (Fig. 3a). Inorganic phosphate was confirmed to be involved in the inorganic phosphate transport system by treatment with foscarnet, an inhibitor of inorganic phosphate transport. As shown in Figure 3b, the mineralized nodule formation of MPDL22 was blocked by foscarnet, suggesting the necessity of transportation of inorganic phosphate for biomineralization by MPDL22.

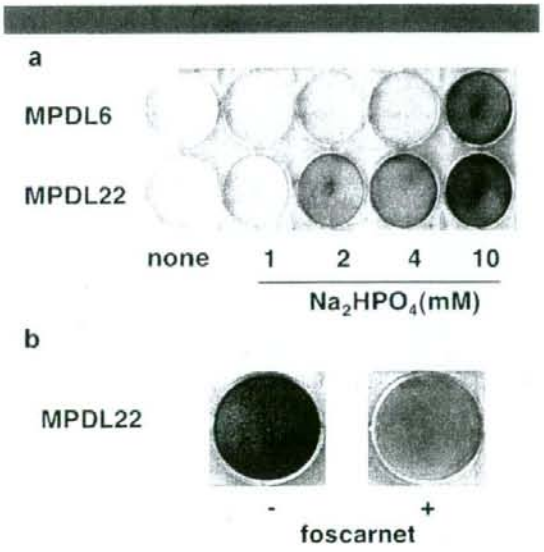

Fig. 3. Involvement of inorganic phosphate on mineralization by MPDL6 and MPDL22. MPDL6 and MPDL22 were cultured for 7 days in the presence or absence of Na_2HPO_4 (1–10 mM) (a) or with or without foscarnet (600 μM) in the presence of Na_2HPO_4 (10 mM) (b). MPDL22 were cultured for 21 days with or without foscarnet (600 μM) in the presence of Na_2PO_4 (10 mM). Mineralized nodules of the cell monolayers were detected with Arizarin red staining as described in "Materials and Methods Section." Results of one representative experiment out of three separate experiments are shown. [Color figure can be viewed in the online issue, which is available at www.interscience.wiley.com.]

Then, we investigated whether inorganic phosphate regulates the expression of osteopontin in MPDL22 and MPDL6. Western blot analysis revealed that treatment of MPDL22 with inorganic phosphate resulted in the enhancement of expression of osteopontin in a dose-dependent manner (Fig. 4a) and that the inorganic phosphate-induced expression of osteopontin was also inhibited with foscarnet (Fig. 4b). In contrast to MPDL22, inorganic phosphate-treated MPDL6 exhibited low expression of osteopontin. A histochemical study also demonstrated abrogation of the elevation of inorganic phosphate-dependent osteopontin in MPDL6 and MPDL22 by foscarnet (Fig. 4c). Thus, inorganic phosphate upregulated the expression of osteopontin in association with the mineralization process by MPDL22 in vitro.

FGF-2 promotes osteopontin and its gene expression in MPDL22

We then examined the effect of FGF-2 on mRNA expression of bone-related molecules in MPDL22. While FGF-2 suppressed mRNA expression of bone-related molecules such as type I collagen, Pebp2αA/Cbfa1, Osf-2/Til-1/Cbfa-1, bone sialoprotein, osteonectin, and osteocalcin, expression of osteopontin was notably elevated in FGF-2-stimulated MPDL22 at both mRNA and protein levels in a dose-dependent manner (Figs. 5 and 6a,c). In contrast, MPDL6 exhibited relatively weak or little expression of osteopontin (Fig. 6b,d). Interestingly, western blot analysis revealed two osteopontin proteins showing slightly different molecular sizes (Fig. 6c,d), which probably suggests the stimulation-dependent posttranslational modification of osteopontin (Denhardt et al., 2001a) since

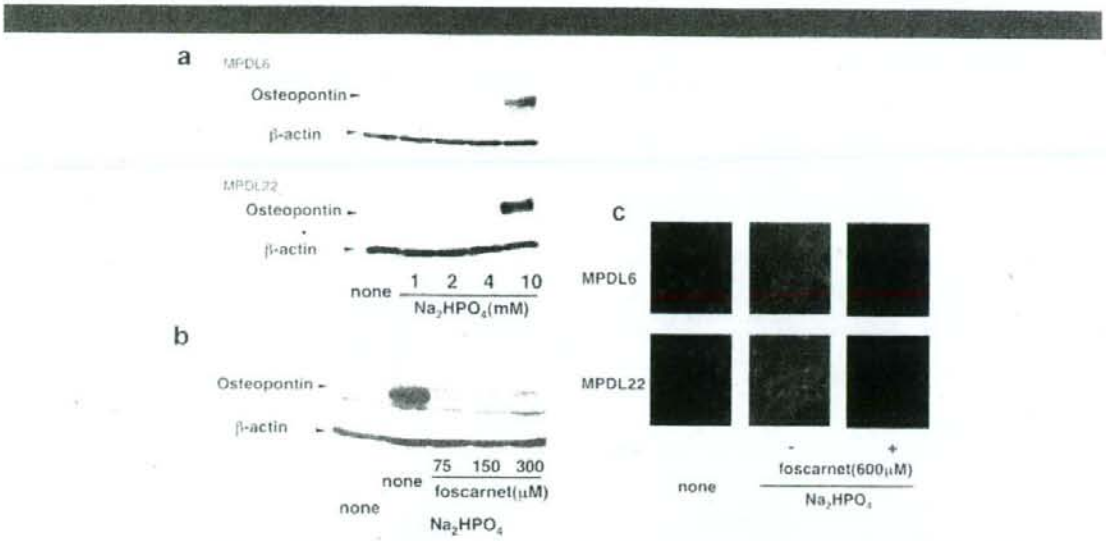

Fig. 4. Involvement of inorganic phosphate in expression of osteopontin by MPDL6 and MPDL22. MPDL6 or MPDL22 was cultured for 48 h in the presence or absence of Na_2HPO_4 (1–10 mM) (a) or with or without foscarnet at indicated concentration in the presence of Na_2HPO_4 (10 mM) (b,c). Samples were electrophoresed on 8% mini-gels, transblotted onto nitrocellulose membrane and immunoreactive osteopontin was detected using a primary goat anti-osteopontin antibody and chemiluminece kit. β-actin was used as an internal control (a,b). Cell monolayers were fixed with 2% paraformaldehyde and incubated with or without anti-osteopontin polyclonal antibody following Alexa Fluor 488 conjugated anti-goat IgG antibody (c). Results of one representative experiment out of three separate experiments are shown.

alternative splicing of osteopontin in mice has not been reported.

FGF-2 but not inorganic phosphate upregulated osteopontin secretion in culture supernatants

Osteopontin functions differently at different sites of localization. Extracellular osteopontin in soluble form plays an important role in cell survival (Rogers et al., 1997; Scatena et al., 1998; Ophascharoensuk et al., 1999; Denhardt et al., 2001a; Lin and Yang-Yen, 2001; Rittling et al., 2002), chemotaxis and migration (Senger et al., 1996; Li et al., 2000) and cell proliferation and invasion (Castellone et al., 2004) via cell surface receptors. Thus, we quantitated the production of osteopontin in culture supernatants of FGF-2- and inorganic phosphate-activated MPDL22. Treatment of MPDL22 with FGF-2 for 48 h markedly enhanced osteopontin secretion in the culture supernatant (Fig. 7). Consistent with the data of MPDL6 shown previously, exposure of MPDL6 to FGF-2 exhibited a slight elevation of osteopontin in the culture supernatant. Interestingly, however, inorganic phosphate rather inhibited the osteopontin production in culture supernatant of either MPDL6 or MPDL22 (Fig. 7). Taken together, these results suggest that osteopontin induced by FGF-2 was localized in a manner different from that induced by inorganic phosphate.

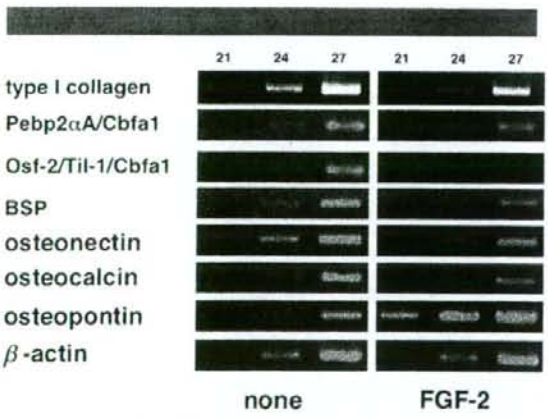

Fig. 5. Effects of FGF-2 on bone-related proteins by MPDL22. MPDL22 was cultured without or with FGF-2 (100 ng/ml) for 24 h. Total mRNA was isolated and RT-PCR was performed to examine the mRNA expression of type I collagen, Pebp2αA/Cbfa1, Osf-2/Til-1/Cbfa1, bone sialoprotein (BSP), osteonectin, osteocalcin, osteopontin, and β-actin in MPDL22. Results of one representative experiment out of three separate experiments are shown. The numbers of PCR cycles used to amplify each mRNA in MPDL22 are shown above each lane.

FGF-2 evoked expression of osteopontin in the cytosol, but not on the cell surface of MPDL

FGF-2, which reversibly suppressed cell differentiation into hard tissue, stimulated MPDL22 to secrete osteopontin. The localization of FGF-2-induced osteopontin in MPDL was determined by histochemical analysis. Unexpectedly, no staining was detectable on the cell surface of both MPDL6 and MPDL22 stimulated with FGF-2, while inorganic phosphate vigorously activated expression of osteopontin on the cell surface (Fig. 8). Recently, osteopontin has been reported to be present not only in the extracellular matrix but also in perinuclear cytosol (Zohar et al., 1997). Thus, in order to detect the intracellular localization of osteopontin, permeabilized cells were stained with anti-osteopontin antibody. Forty-eight hours after FGF-2 stimulation, weak punctuate immunostaining pattern was detected in perinuclear cytoplasm of the MPDL22 (Fig. 9). In the permeabilized-cell experiment, MPDL6 expressed osteopontin at a lower level

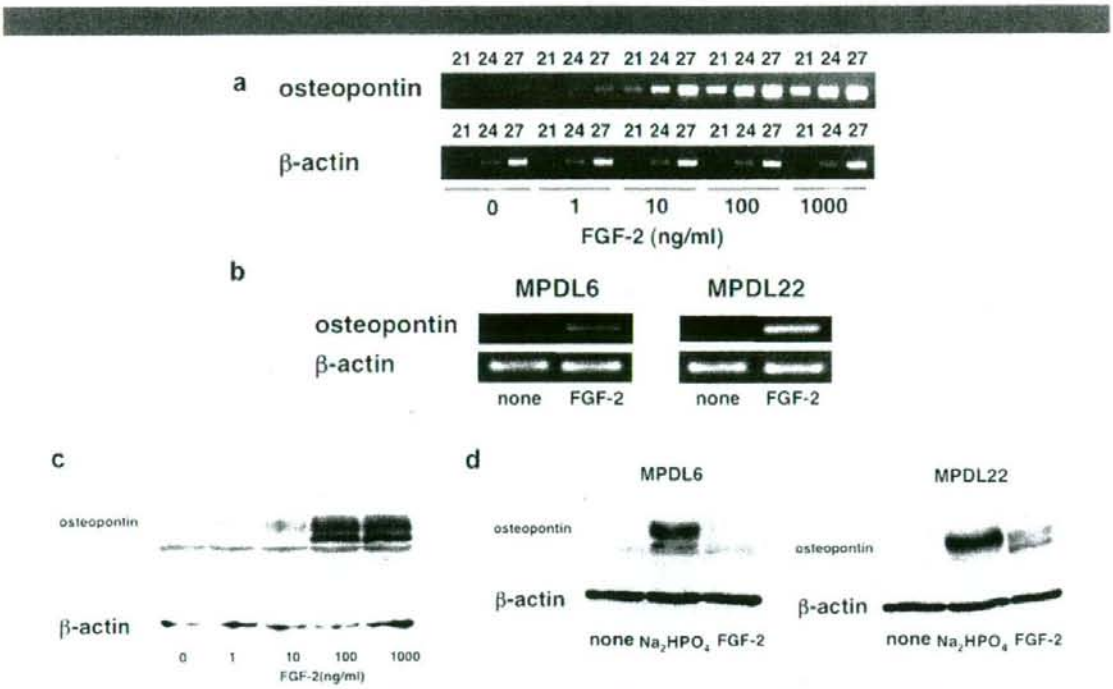

Fig. 6. Effects of FGF-2 on expression of osteopontin by MPDL6 and MPDL22. MPDL22 was cultured without or with FGF-2 (1–1,000 ng/ml) (a,c). In another experiment, MPDL6 and MPDL22 were cultured without or with FGF-2 (100 ng/ml) (b,d) or with Na_2HPO_4 (10 mM) (d). After 24 h of incubation, total mRNA was isolated from each cell and RT-PCR was performed to examine the mRNA expression of osteopontin, β-actin in MPDL6 (b) and MPDL22 (a,b). The numbers of PCR cycles used to amplify each mRNA in the MPDL cells are shown above each lane. Results of one representative experiment out of three separate experiments are shown. After 48 h of culture, protein was extracted as described in "Materials and Methods Section." Samples were electrophoresed on 8% mini-gels, transblotted onto nitrocellulose membrane and immunoreactive osteopontin was detected using a primary goat anti-osteopontin antibody and chemiluminescence kit (c,d). β-actin was used as an internal control (c,d). Results of one representative experiment out of three separate experiments are shown.

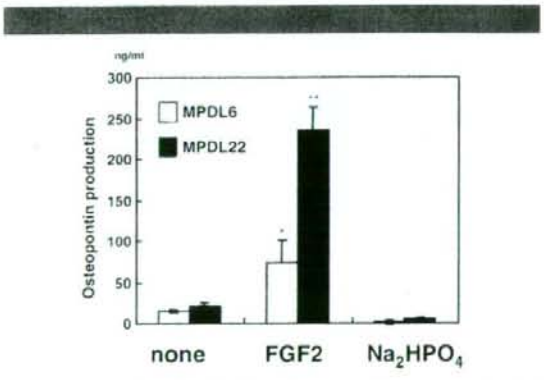

Fig. 7. Osteopontin production in culture supernatant of MPDL6 or MPDL22 in response to FGF-2 or inorganic phosphate stimulation. MPDL6 and MPDL22 were cultured as described in "Materials and Methods Section." Culture supernatants were removed after 48 h of culture and the concentration of osteopontin in the conditioned medium was determined by an ELISA assay as described in "Materials and Methods Section" ($^*P < 0.05$ and $^{**}P < 0.01$ compared to unstimulated control). Results are expressed as the mean ± SD of three separate experiments.

than that of MPDL22. As in the case of MPDL22, without permeabilization, no staining was observed on FGF-2-stimulated MPDL6. In contrast, inorganic phosphate induced strong expression of osteopontin on non-permeabilized and permeabilized MPDL6 and MPDL22.

The localization of osteopontin in cytosol- or membrane-associated fraction of MPDL22 in response to FGF-2 or inorganic phosphate was further examined by western blot analysis. The biochemical analysis revealed that FGF-2 increased the expression of osteopontin in the cytosol but not in the membrane-associated fraction whereas inorganic phosphate enhanced the expression of osteopontin in both fractions (particularly in the cytosol fraction) (Fig. 10).

Osteopontin interacts with other extracellular matrices such as collagen and fibronectin on the cell surface (Aeschlimann et al., 1993, 1995; Heath et al., 2001). Thus, membrane-associated osteopontin which was observed in inorganic phosphate-induced MPDL22 may interact with such extracellular matrices on the cell surface. To test this possibility, double stainings of osteopontin/collagen and osteopontin/fibronectin in inorganic phosphate-stimulated MPDL22 were conducted. Unstimulated MPDL22 showed weak expression of osteopontin, collagen type I and fibronectin (data not shown). Activation of MPDL22 with inorganic phosphate elucidated the increased level of these matrices (Fig. 11a,b,e,f). Co-localization of osteopontin with collagen type I and, notably, with fibronectin was observed (Fig. 11d,h). In addition, treatment of

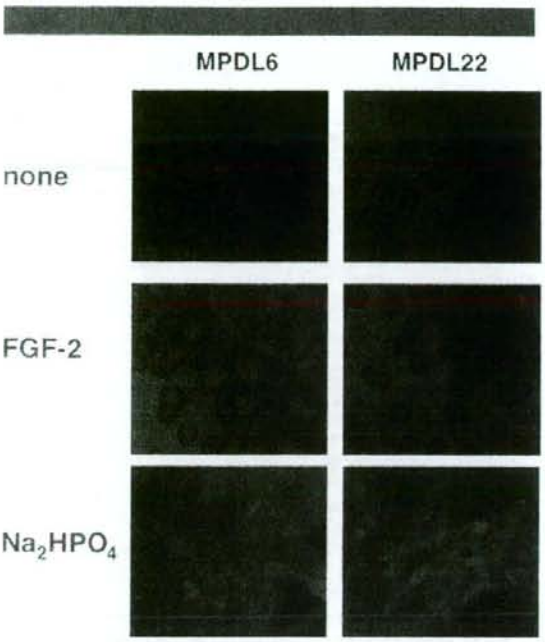

Fig. 8. Expression of osteopontin on MPDL6 or MPDL22 in response to FGF-2 or inorganic phosphate stimulation. MPDL6 and MPDL22 were cultured for 48 h in the presence or absence of FGF-2 (100 ng/ml) or Na_2HPO_4 (10 mM). Each cell monolayer was fixed with 2% paraformaldehyde and incubated with or without anti-osteopontin polyclonal antibody after incubation with Alexa Fluor 488 conjugated anti-goat IgG antibody. Results of one representative experiment out of three separate experiments are shown.

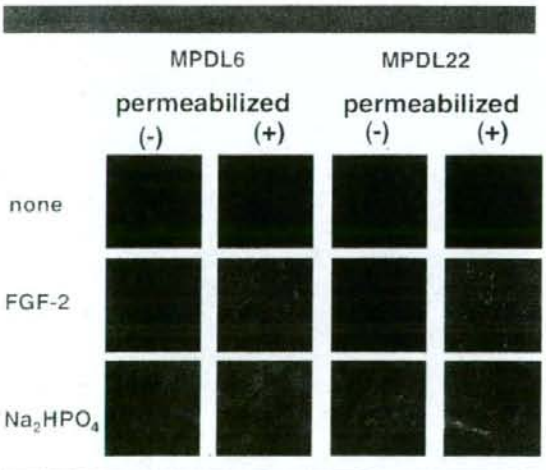

Fig. 9. Expression of osteopontin of permeabilized MPDL6 or MPDL22 in response to FGF-2 or inorganic phosphate stimulation. MPDL6 and MPDL22 were cultured for 48 h in the presence or absence of FGF-2 (100 ng/ml) or Na_2HPO_4 (10 mM). Each cell monolayer was fixed with 2% paraformaldehyde or 2% paraformaldehyde combined with 0.1% Triton X to permeabilize the monolayers and incubated with or without anti-osteopontin polyclonal antibody after incubation with Alexa Fluor 488 conjugated anti-goat IgG antibody. Results of one representative experiment out of three separate experiments are shown.

inorganic phosphate-stimulated MPDL22 with collagenase resulted in the prominent reduction of not only collagen but also osteopontin expressions of MPDL22 (data not shown). As a control, hyaluronidase treatment abrogated the expression of hyaluronan, but not that of osteopontin. These results suggest that osteopontin was anchored on the cell surface probably via collagen and fibronectin matrices.

Soluble osteopontin promoted cell survival of MPDL22

Soluble osteopontin interacts with several cell-surface receptors and modulates various cell functions. Osteopontin has been reported to promote the survival of endothelial cells (Scatena et al., 1998; Khan et al., 2002), epithelial cells (Rogers et al., 1997; Ophascharoensuk et al., 1999), and vascular smooth muscle cells (Weintraub et al., 2000). As shown in Figure 12, the conditioned medium of FGF-2-stimulated MPDL22 suppressed the apoptosis. The suppressive effect was partially but significantly inhibited by neutralizing anti-osteopontin antibody (Fig. 12). Although FGF-2 also has an anti-apoptotic effect (Debiais et al., 2004), the anti-FGF-2 neutralizing antibody did not alter the survival effect of the culture supernatant of FGF-2-stimulated MPDL22 (data not shown).

Discussion

In this study, we demonstrated that the localization and expression pattern of the osteopontin induced by inorganic phosphate and that induced by FGF-2 were different. Of interest, inorganic phosphate enhanced the formation of mineralized nodules via its influx into cells (Fig. 3), while FGF-2 suppressed it (Takayama et al., 1997). Osteopontin is an abundant acidic glycoprotein present in extracellular matrix of mineralized tissue albeit negatively related to mineralization (Ishijima et al., 2007). This suggests that the inorganic phosphate-induced osteopontin is probably relevant to regulation of mineralization. In contrast, osteopontin was not expressed on the cell surface but osteopontin secretion was elevated in the culture supernatant by MPDL22 in response to FGF-2 (Fig. 7). This implies that FGF-2-induced osteopontin may be associated with function(s) distinct from biomineralization.

Since osteopontin is unable to form organized multimeric structures, its interaction with other extracellular molecules is essential for its association with the insoluble extracellular matrix. Osteopontin binds extracellular matrices such as collagen, fibronectin, and osteocalcin and therefore interacts with the hydroxyapatite crystal with high affinity (Singh et al., 1990; Boskey et al., 1993; Kaartinen et al., 1999; Weintraub et al., 2000). Cell surface-associated fibronectin is capable of bind to osteopontin as heat-dissociable cross-linked products likely by effects of transglutaminase (Mukherjee et al., 1995). Therefore, an appropriate tight association of osteopontin with other extracellular matrices may be critical for its localization on cell surface. As shown in Figure 11, osteopontin is co-localized predominantly with fibronectin and partially with collagen. And collagenase treatment, which decreased the expression of collagen and fibronectin in inorganic phosphate-stimulated MPDL22, resulted in partial reduction of expression of osteopontin, while hyaluronidase treatment did not (data not shown). These results suggest that fibronectin and/or collagen, at least partially, mediates the osteopontin adhesion on cell surface and that expression of osteopontin on the cell surface is attributed to collagen-fibronectin complex. On the other hand, FGF-2 suppressed the expression of type I collagen by human PDL cells and MPDL 22 (Takayama et al., 1997). These results suggest the impaired adherence of FGF-2-induced osteopontin to the extracellular matrix on the cell surface. Taken together, the difference of extracellular

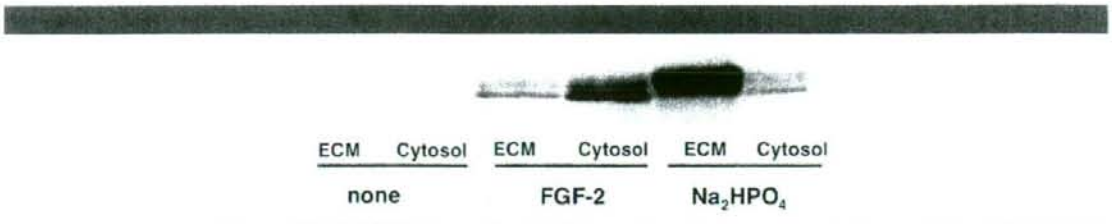

Fig. 10. Expression of osteopontin in cytosol or plasma membrane fraction of MPDL22 in response to FGF-2 or inorganic phosphate stimulation. MPDL22 (1×10^5), which had been cultured for 48 h in the presence or absence of FGF-2 (100 ng/ml) or inorganic phosphate (10 mM), were collected, homogenized on ice and centrifuged at 700*g* for 10 min at 4°C. The supernatant and pellet were used as the cytosol fraction and plasma membrane protein, respectively. Each fraction was subjected to western blot analysis as described in "Materials and Methods Section." Results of one representative experiment out of three separate experiments are shown.

matrix expression of MPDL22 in response to the stimulation with inorganic phosphate and FGF-2 may, in part, account for the distinct localization of osteopontin.

Osteopontin bound to the cell surface is phosphorylated and forms a heat-stable complex with fibronectin, while dephosphorylated osteopontin forms a heat-dissociable complex with fibronectin in culture supernatant (Singh et al., 1990). Furthermore, the inhibitory effect of osteopontin on mineralization was found to depend on the phosphorylation of osteopontin (Jono et al., 2000; Pampena et al., 2004). In this study, western blot analysis revealed a slight difference in molecular size between cell-surface-associated osteopontin and that detected in the culture supernatant (Fig. 10). This difference may be explained by posttranslational modification. Post-translational modification of osteopontin, such as phosphorylation, *N*- and *O*-glycosylation, and transglutaminase catalyzation contributes to its interaction with other extracellular matrices. Such interactions are thought to be necessary for bone mineralization (Glimcher, 1989; Saavedra, 1994; Sorensen and Petersen, 1995). Unfortunately, however, western blotting analysis revealed similar immunoreactive staining with anti-phosphotyrosine excluding anti-phosphoserine and anti-phosphothreonine antibodies in both FGF-2- and inorganic phosphate-induced osteopontin (data not shown). In addition, *N*- and *O*-glycosidase treatment did not cause a prominent effect on molecular weight and exposure of tissue transglutaminase to FGF-2-activated MPDL22 unchanged expression of osteopontin on the cell surface (data not shown). Further investigation regarding other modifications affecting the property of osteopontin is needed.

Osteopontin is detected within cementum surface and PDL cells (McKee and Nanci, 1996; Lao et al., 2006) and implicated in cementogenesis and homeostasis of periodontal tissues (MacNeil et al., 1995a,b). Interestingly, increased gene expression of osteopontin in cementoblast was observed following stimulation with inorganic phosphate while collagen type I mRNA was decreased (Foster et al., 2006) and the effects were inhibited by the treatment of cementoblast with foscarnet. FGF-2 increased DNA synthesis and osteopontin expression but decreased gene expression of osteocalcin and

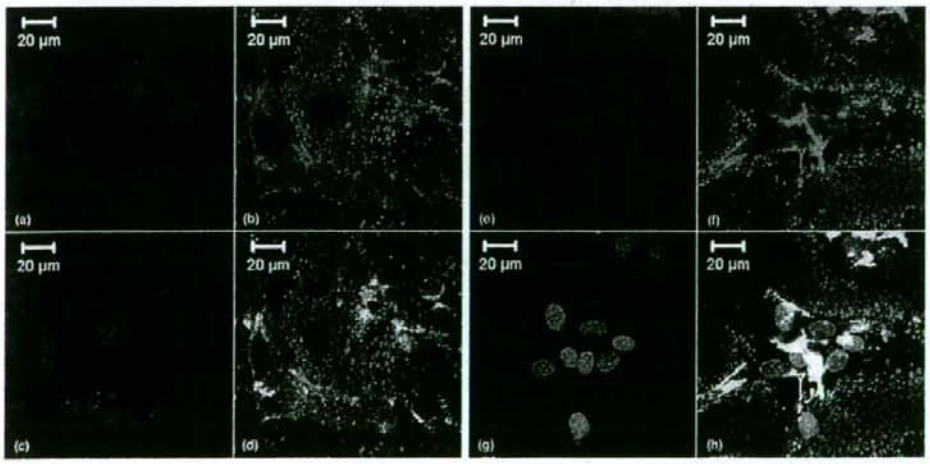

Fig. 11. Extracellular matrix expression of MPDL22 in response to inorganic phosphate stimulation. MPDL22 was cultured for 48 h in the presence of Na_2HPO_4 (10 mM). Cell monolayers were fixed with 2% paraformaldehyde and incubated with or without goat anti-osteopontin antibody (b,f), rabbit anti-Type I collagen (a) or anti-fibronectin (e) polyclonal antibody after incubation with Alexa Fluor 488 conjugated anti-goat IgG antibody (b,f) or Alexa Fluor 546 goat anti-rabbit IgG (a,e). DAPI staining was performed to stain nuclear (c,g). Parts (a–c) and (e–g) were merged into parts (d) and (h), respectively. Incubation of inorganic phosphate-stimulated MPDL22 with Alexa Fluor 488 conjugated anti-goat IgG antibody or Alexa Fluor 546 goat anti-rabbit IgG did not result in any staining. Results of one representative experiment out of three separate experiments are shown.

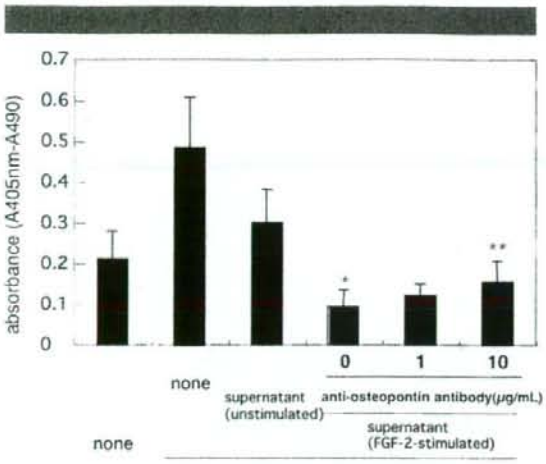

Fig. 12. Suppressive effect of FGF-2-induced osteopontin on apoptosis. Apoptosis was detected using a cell death detection ELISA^{plus} kit following the instruction manual. MPDL22 was treated with 2 μg/ml of camptothecin for 4 h at 37°C to induce apoptosis. The cells were lysed with lysis buffer and the lysate was centrifuged. Twenty microliter from the supernatant was transferred into the streptoavidin-coated 96-well plate and anti-histone-biotin and anti DNA-peroxidase were added to each well, incubated for 2 h. Color was developed with ABTS solution and absorbance was measured using a microplate reader (*$P < 0.05$ compared to unstimulated control, **$P < 0.05$ compared to culture without anti-osteopontin antibody). Results are expressed as the mean ± SD of three separate experiments.

bone sialoprotein with suppression of mineral nodule formation by cementoblast (Hakki et al., 2005). These results including our data suggest that mouse cementoblasts as well as MPDL22 are influenced by inorganic phosphate and FGF-2 to regulate expression of bone-related extracellular matrices. In contrast, FGF-2 stimulated osteocalcin mRNA and promoter activity with increased Runx2 phosphorylation in MC3T3-E1 preosteoblastic cells (Xiao et al., 2002). This indicates that effects of FGF-2 on hard tissue formation and mineralization may differ between each cell type. Similarly, functions of osteopontin appear to vary depending on the cell types despite mineralizing and non-mineralizing tissue.

Osteopontin is produced by injured epithelium and inflammatory infiltrates (Murry et al., 1994; O'Brien et al., 1994; Nau et al., 1997; Liaw et al., 1998; O'Regan et al., 1999). In addition, osteopontin promotes the survival of epithelial cells exposed to injury (Noiri et al., 1999; Denhardt et al., 2001b). A recent study using osteopontin knock-out mice has revealed abnormal matrix organization during skin incisinal wound healing (Liaw et al., 1998). In this study, we demonstrated that FGF-2-induced osteopontin played roles in cell survival (Fig. 12) and migration of MPDL22 (data not shown). FGF-2 also activated cranial suture closure of cultured mouse calvaria with increased expression of osteopontin (Kim et al., 2003). Furthermore, the FGF-2-induced osteopontin amplified neovascularization via osteopontin-mediated recruitment of proangiogenic monocytes (Leali et al., 2003) and endothelial cell survival (Scatena et al., 1998; Khan et al., 2002). Interestingly, topical application of FGF-2 to experimentally induced periodontitis sites with alveolar bone defects prompted periodontal tissue regeneration. FGF-2 has been suggested to induce proliferation of PDL cells, modulation of extracellular matrix production (Takayama et al., 1997) and angiogenesis, and thereby accelerates periodontal regeneration (Murakami et al., 1999). Taken together, these findings suggest that FGF-2-induced osteopontin is associated with the early phase of wound healing and that it shows beneficial and cross-talk effects with FGF-2 during the course of periodontal tissue regeneration.

Increased osteopontin levels have been demonstrated in inflammatory disease (Denhardt and Guo, 1993; Nau et al., 2000; Hashimoto et al., 2003; Leali et al., 2003; Agnholt et al., 2007), such as rheumatic heart valves (Rajamannan et al., 2005), pulmonary inflammation (Takahashi et al., 2001) and Crohn's disease (Agnholt et al., 2007). Numerous factors including phorbol esters, concanavalin A, and various growth factors and cytokines, such as IL-1, IL-2, IL-3, LPS, TNF-α, BMP, EGF, FGF-2, TGF-β, and PDGF, up-regulated osteopontin production (Denhardt and Guo, 1993; Denhardt and Noda, 1998; O'Regan and Berman, 2000). Osteopontin inhibits NO production and iNOS expression (Rollo et al., 1996; Guo et al., 2001) and regulates production of a variety of cytokines by T cells, monocytes and macrophages (Ashkar et al., 2000; Naldini et al., 2006; Agnholt et al., 2007). Moreover, osteopontin augmented the mitgenic action of PDGF (Takahashi et al., 2001). These results suggest that osteopontin contributes to regulate inflammatory response and subsequent tissue remodeling through cell adhesion, chemotaxis, cytokine regulation, and prevention of apoptosis (Hijiya et al., 1994; O'Regan and Berman, 2000; Denhardt et al., 2001b).

Osteopontin-deficient mice exhibit less accumulation of macrophage in inflammation in ischemic kidneys (Persy et al., 2003) and the abnormal wound repair (Liaw et al., 1998). Osteopontin expression was associated with infiltration and migration of T cell and monocytes (Patarca et al., 1989; Giachelli et al., 1994; O'Regan et al., 1999). It has been reported that chemotactic factor for monocyte infiltration and proinflammatory cytokines expression contribute proangiogenic activity of osteopontin (Leali et al., 2003; Naldini et al., 2006). Furthermore, osteopontin function as mediator of cell migration, chemotactic factor for macrophage and muscle cells (Liaw et al., 1994; Bendeck et al., 2000). Perimembranous osteopontin co-localization with CD44 was observed at leading edge in migrating fibroblasts (Zohar et al., 2000). Similarly, perinuclear osteopontin was present in migratory MPDL22 and its expression and CD44 expression was enhanced by stimulation with FGF-2 (data not shown). Identification of other functions of osteopontin in FGF-2-stimulated MPDL22 is thus of paramount interest in future studies.

Osteopontin can bind to several receptors including integrin $\alpha_v\beta1$, $\alpha_v\beta3$, $\alpha_v\beta5$, $\alpha4\beta1$, $\alpha4\beta5$, $\alpha8\beta1$, $\alpha9\beta1$, and certain variant forms of CD44 (Denhardt et al., 2001b). CD44 and $\alpha_v\beta3$ has been reported to mediate cell motility (Chellaiah and Hruska, 2003). In particular, the interaction of osteopontin with the cell surface receptor CD44 has been reported to elicit a cell survival response and phosphatidylinositol 3-kinase/AKT signaling pathway accounted for its function (Lin et al., 2000; Lin and Yang-Yen, 2001). Interestingly, treatment of MPDL22 with FGF-2 resulted in an increase in the level of CD44 expression. This suggests that CD44 on MPDL22 is related to the osteopontin-dependent motility. Further investigation on this matter is now in progress.

The present study revealed that inorganic phosphate and FGF-2 differentially regulate the expression of osteopontin by PDL cells. These observations provide important insight into the roles of osteopontin in not only the late phase (mineralization) but also the early phase (cell proliferation, survival, and migration) of the periodontal regeneration process caused by PDL cells, although additional studies are necessary to delineate the detail functions of osteopontin released in response to FGF-2.

Acknowledgments

This work was supported in part by Grants-in-Aid for Scientific Research (No. 16209056, No. 17209065, No. 17390560, No. 17390561 and No. 18890107) and the 21st Century COE entitled "Origination of Frontier BioDentistry" at Osaka University Graduate School of Dentistry supported by the Ministry of Education, Culture, Sports, Science and Technology.

Literature Cited

Aeschlimann D, Wetterwald A, Fleisch H, Paulsson M. 1993. Expression of tissue transglutaminase in skeletal tissues correlates with events of terminal differentiation of chondrocytes. J Cell Biol 120:1461–1470.

Aeschlimann D, Kaupp O, Paulsson M. 1995. Transglutaminase-catalyzed matrix cross-linking in differentiating cartilage: Identification of osteonectin as a major glutaminyl substrate. J Cell Biol 129:881–892.

Agnholt J, Kelsen J, Schack L, Hvas CL, Dahlerup JF, Sørensen ES. 2007. Osteopontin, a protein with cytokine-like properties, is associated with inflammation in Crohn's disease. Scand J Immunol 65:453–460.

Ashkar S, Weber GF, Panoutsakopoulou V, Sanchirico ME, Jansson M, Zawaideh S, Rittling SR, Denhardt DT, Glimcher MJ, Cantor H. 2000. Eta-1 (osteopontin): An early component of type-1 (cell-mediated) immunity. Science 287:860–864.

Beck GRJ, Moran E, Knecht N. 2003. Inorganic phosphate regulates multiple genes during osteoblast differentiation, including Nrf2. Exp Cell Res 288:288–300.

Bellows CG, Heersche JN, Aubin JE. 1992. Inorganic phosphate added exogenously or released from beta-glycerophosphate initiates mineralization of osteoid nodules in vitro. Bone Miner 17:15–29.

Bendeck MP, Irvin C, Reidy M, Smith L, Mulholland D, Horton M, Giachelli CM. 2000. Smooth muscle cell matrix metalloproteinase production is stimulated via alpha(v)beta(3) integrin. Arterioscler Thromb Vasc Biol 20:1467–1472.

Bessey OA, Lowry OH. 1946. A method for rapid determination of alkaline phosphatase with five cubic millimeters of serum. J Biol Chem 164:321–329.

Boskey AL, Maresca M, Ullrich W, Doty SB, Butler WT, Prince CW. 1993. Osteopontin-hydroxyapatite interactions in vitro: Inhibition of hydroxyapatite formation and growth in a gelatin-gel. Bone Miner 22:147–159.

Castellone MD, Celetti A, Guarino V, Cirafici AM, Basolo F, Giannini R, Medico E, Kruhoffer M, Orntoft TF, Curcio F, Fusco A, Melillo RM, Santoro M. 2004. Autocrine stimulation by osteopontin plays a pivotal role in the expression of the mitogenic and invasive phenotype of RET/PTC-transformed thyroid cells. Oncogene 23:2188–2196.

Chellaiah MA, Hruska KA. 2003. The integrin alpha(v)beta(3) and CD44 regulate the actions of osteopontin on osteoclast motility. Calcif Tissue Int 72:197–205.

Chung CH, Golub EE, Forbes ETT, Shapiro IM. 1992. Mechanism of action of beta-glycerophosphate on bone cell mineralization. Calcif Tissue Int 51:305–311.

Dahl LK. 1952. A simple and sensitive histochemical method for calcium. Proc Soc Exp Biol Med 80:474–479.

Debiais F, Lefevre G, Lemonnier J, Le Mee S, Lasmoles F, Mascarelli F, Marie PJ. 2004. Fibroblast growth factor-2 induces osteoblast survival through a phosphatidylinositol 3-kinase-dependent, -beta-catenin-independent signaling pathway. Exp Cell Res 297:235–246.

Denhardt DT, Guo XJ. 1993. Osteopontin: A protein with diverse functions. FASEB J 7:1475–1482.

Denhardt DT, Noda M. 1998. Osteopontin expression and function: Role in bone remodeling. J Cell Biochem Suppl 30–31:92–102 (Review).

Denhardt DT, Giachelli CM, Rittling SR. 2001a. Role of osteopontin in cellular signaling and toxicant injury. Annu Rev Pharmacol Toxicol 41:723–749.

Denhardt DT, Noda M, O'Regan AW, Pavlin D, Berman JS. 2001b. Osteopontin as a means to cope with environmental insults: Regulation of inflammation, tissue remodeling, and cell survival. J Clin Invest 107:1055–1061.

Foster BL, Nociti FHJ, Swanson EC, Matsa-Dunn D, Berry JE, Cupp CJ, Zhang P, Somerman MJ. 2006. Regulation of cementoblast gene expression by inorganic phosphate in vitro. Calcif Tissue Int 78:103–112.

Giachelli CM, Pichler R, Lombardi D, Denhardt DT, Alpers CE, Schwartz SM, Johnson RJ. 1994. Osteopontin expression in angiotensin II-induced tubulointerstitial nephritis. Kidney Int 45:515–524.

Glimcher MJ. 1989. Mechanism of calcification: Role of collagen fibrils and collagen-phosphoprotein complexes in vitro and in vivo. Anat Rec 224:139–153.

Guo H, Cai CQ, Schroeder RA, Kuo PC. 2001. Osteopontin is a negative feedback regulator of nitric oxide synthesis in murine macrophages. J Immunol 166:1079–1086.

Hakki SS, Nohutcu RM, Hakki EE, Berry JE, Akkaya MS, Somerman MJ. 2005. Dexamethasone and basic-fibroblast growth factor regulate markers of mineralization in cementoblasts in vitro. J Periodontol 76:1550–1558.

Hashimoto M, Koda M, Ino H, Murakami M, Yamazaki M, Moriya H. 2003. Upregulation of osteopontin expression in rat spinal cord microglia after traumatic injury. J Neurotrauma 20:287–296.

Heath DJ, Downes S, Verderio E, Griffin M. 2001. Characterization of tissue transglutaminase in human osteoblast-like cells. J Bone Miner Res 16:1477–1485.

Hijiya N, Setoguchi M, Matsuura K, Higuchi Y, Akizuki S, Yamamoto S. 1994. Cloning and characterization of the human osteopontin gene and its promoter. Biochem J 303:255–262.

Ishijima M, Tsuji K, Rittling SR, Yamashita T, Kurosawa H, Denhardt DT, Nifuji A, Ezura Y, Noda M. 2007. Osteopontin is required for mechanical stress-dependent signals to bone marrow cells. J Endocrinol 193:235–243.

Jono S, Peinado C, Giachelli CM. 2000. Phosphorylation of osteopontin is required for inhibition of vascular smooth muscle cell calcification. J Biol Chem 275:20197–20203.

Kaartinen MT, Pirhonen A, Linnala-Kankkunen A, Maenpaa PH. 1999. Cross-linking of osteopontin by tissue transglutaminase increases its collagen binding properties. J Biol Chem 274:1729–1735.

Khan SA, Lopez-Chua CA, Zhang J, Fisher LW, Sorensen ES, Denhardt DT. 2002. Soluble osteopontin inhibits apoptosis of adherent endothelial cells deprived of growth factors. J Cell Biochem 85:728–736.

Kim HJ, Lee MH, Park HS, Park MH, Lee SW, Kim SY, Choi JY, Shin HI, Kim HJ, Ryoo HM. 2003. Erk pathway and activator protein 1 play crucial roles in FGF2-stimulated premature cranial suture closure. Dev Dyn 227:335–346.

Labarca C, Paigen K. 1980. A simple, rapid, and sensitive DNA assay procedure. Anal Biochem 102:344–352.

Lao M, Marino V, Bartold PM. 2006. Immunohistochemical study of bone sialoprotein and osteopontin in healthy and diseased root surfaces. J Periodontol 77:1665–1673.

Leali D, Dell'Era P, Stabile H, Sennino B, Chambers AF, Naldini A, Sozzani S, Nico B, Ribatti D, Presta M. 2003. Osteopontin (Eta-1) and fibroblast growth factor-2 cross-talk in angiogenesis. J Immunol 171:1085–1093.

Li G, Chen YF, Kelpke SS, Oparil S, Thompson JA. 2000. Estrogen attenuates integrin-beta(3)-dependent adventitial fibroblast migration after inhibition of osteopontin production in vascular smooth muscle cells. Circulation 101:2949–2955.

Liaw L, Almeida M, Hart CE, Schwartz SM, Giachelli CM. 1994. Osteopontin promotes vascular cell adhesion and spreading and is chemotactic for smooth muscle cells in vitro. Circ Res 74:214–224.

Liaw L, Birk DE, Ballas CB, Whitsitt JS, Davidson JM, Hogan BL. 1998. Altered wound healing in mice lacking a functional osteopontin gene (spp1). J Clin Invest 101:1468–1478.

Lin YH, Yang-Yen HF. 2001. The osteopontin-CD44 survival signal involves activation of the phosphatidylinositol 3-kinase/Akt signaling pathway. J Biol Chem 276:46024–46030.

Lin YH, Huang CJ, Chao JR, Chen ST, Lee SF, Yen JJ, Yang-Yen HF. 2000. Coupling of osteopontin and its cell surface receptor CD44 to the cell survival response elicited by interleukin-3 or granulocyte-macrophage colony-stimulating factor. Mol Cell Biol 20:2734–2742.

MacNeil RL, Berry J, D'Errico J, Strayhorn C, Piotrowski B, Somerman MJ. 1995a. Role of two mineral-associated adhesion molecules, osteopontin and bone sialoprotein, during cementogenesis. Connect Tissue Res 33:1–7 (Review).

MacNeil RL, Berry J, D'Errico J, Strayhorn C, Somerman MJ. 1995b. Localization and expression of osteopontin in mineralized and nonmineralized tissues of the periodontium. Ann N Y Acad Sci 760:166–176 (Review).

McKee MD, Nanci A. 1996. Secretion of Osteopontin by macrophages and its accumulation at tissue surfaces during wound healing in mineralized tissues: A potential requirement for macrophage adhesion and phagocytosis. Anat Rec 245:394–409.

Mukherjee BB, Nemir M, Beninati S, Cordella-Miele E, Singh K, Chackalaparampil I, Shanmugam V, DeVouge MW, Mukherjee AB. 1995. Interaction of osteopontin with fibronectin and other extracellular matrix molecules. Ann N Y Acad Sci 21:201–212.

Murakami S, Takayama S, Ikezawa K, Shimabukuro Y, Kitamura M, Nozaki T, Terashima A, Asano T, Okada H. 1999. Regeneration of periodontal tissues by basic fibroblast growth factor. J Periodontal Res 34:425–430.

Murakami S, Takayama S, Kitamura M, Shimabukuro Y, Yanagi K, Ikezawa K, Saho T, Nozaki T, Okada H. 2003. Recombinant human basic fibroblast growth factor (bFGF) stimulates periodontal regeneration in class II furcation defects created in beagle dogs. J Periodontal Res 38:97–103.

Murry CE, Giachelli CM, Schwartz SM, Vracko R. 1994. Macrophages express osteopontin during repair of myocardial necrosis. Am J Pathol 145:1450–1462.

Naldini A, Leali D, Pucci A, Morena E, Carraro F, Nico B, Ribatti D, Presta M. 2006. IL-1beta mediates the proangiogenic activity of osteopontin-activated human monocytes. J Immunol 177:4267–4270.

Nau GJ, Guilfoile P, Chupp GL, Berman JS, Kim SJ, Kornfeld H, Young RA. 1997. A chemoattractant cytokine associated with granulomas in tuberculosis and silicosis. Proc Natl Acad Sci USA 94:6414–6419.

Nau GJ, Chupp GL, Emile JF, Jouanguy E, Berman JS, Casanova JL, Young RA. 2000. Osteopontin expression correlates with clinical outcome in patients with mycobacterial infection. Am J Pathol 157:37–42.

Noiri E, Dickman K, Miller F, Romanov G, Romanov VI, Shaw R, Chambers AF, Rittling SR, Denhardt DT, Goligorsky MS. 1999. Reduced tolerance to acute renal ischemia in mice with a targeted disruption of the osteopontin gene. Kidney Int 56:74–82.

O'Brien ER, Garvin MR, Stewart DK, Hinohara T, Simpson JB, Schwartz SM, Giachelli CM. 1994. Osteopontin is synthesized by macrophage, smooth muscle, and endothelial cells in primary and restenotic human coronary atherosclerotic plaques. Arterioscler Thromb 14:1648–1656.

Ophascharoensuk V, Giachelli CM, Gordon K, Hughes J, Pichler R, Brown P, Liaw L, Schmidt R, Shankland SJ, Alpers CE, Couser WG, Johnson RJ. 1999. Obstructive uropathy in the mouse: Role of osteopontin in interstitial fibrosis and apoptosis. Kidney Int 56:571–580.

O'Regan A, Berman JS. 2000. Osteopontin: A key cytokine in cell-mediated and granulomatous inflammation. Int J Exp Pathol 81:373–390.

O'Regan AW, Chupp GL, Lowry JA, Goetschkes M, Mulligan N, Berman JS. 1999. Osteopontin is associated with T cells in sarcoid granulomas and has T cell adhesive and cytokine-like properties in vitro. J Immunol 162:1024–1031.

Pampena DA, Robertson KA, Litvinova O, Lajoie G, Goldberg HA, Hunter GK. 2004. Inhibition of hydroxyapatite formation by osteopontin phosphopeptides. Biochem J 378:1083–1087.

Patarca R, Freeman GJ, Singh RP, Wei FY, Durfee T, Blattner F, Regnier DC, Kozak CA, Mock BA, Morse HCI, Jerrells TR, Cantor H. 1989. Structural and functional studies of the early T lymphocyte activation 1 (Eta-1) gene. Definition of a novel T cell-dependent response associated with genetic resistance to bacterial infection. J Exp Med 170:145–161.

Persy VP, Verhulst A, Ysebaert DK, De Greef KE, De Broe ME. 2003. Reduced postischemic macrophage infiltration and interstitial fibrosis in osteopontin knockout mice. Kidney Int 63:543–553.

Rajamannan NM, Nealis TB, Subramaniam M, Pandya S, Stock SR, Ignatiev CI, Sebo JT, Rosengart TK, Edwards WD, McCarthy PM, Bonow RO, Spelsberg TC. 2005. Calcified rheumatic valve neoangiogenesis is associated with vascular endothelial growth factor expression and osteoblast-like bone formation. Circulation 111:3296–3301.

Rittling SR, Chen Y, Feng F, Wu Y. 2002. Tumor-derived osteopontin is soluble, not matrix associated. J Biol Chem 277:9175–9182.

Rogers SA, Padanilam BJ, Hruska KA, Giachelli CM, Hammerman MR. 1997. Metanephric osteopontin regulates nephrogenesis in vitro. Am J Physiol 272:F469–F476.

Rollo EE, Laskin DL, Denhardt DT. 1996. Osteopontin inhibits nitric oxide production and cytotoxicity by activated R AW264.7 macrophages. J Leukoc Biol 60:397.

Saavedra RA. 1994. The roles of autophosphorylation and phosphorylation in the life of osteopontin. Bioessays 16:913–918.

Scatena M, Almeida M, Chaisson ML, Fausto N, Nicosia RF, Giachelli CM. 1998. NF-kappaB mediates alphavbeta3 integrin-induced endothelial cell survival. J Cell Biol 141:1083–1093.

Senger DR, Asch BB, Smith BD, Perruzzi CA, Dvorak HF. 1983. A secreted phosphoprotein marker for neoplastic transformation of both epithelial and fibroblastic cells. Nature 302:714–715.

Senger DR, Ledbetter SR, Claffey KP, Papadopoulos-Sergiou A, Peruzzi CA, Detmar M. 1996. Stimulation of endothelial cell migration by vascular permeability factor/vascular endothelial growth factor through cooperative mechanisms involving the alphavbeta3 integrin, osteopontin, and thrombin. Am J Pathol 149:293–305.

Seo BM, Miura M, Gronthos S, Bartold PM, Batouli S, Brahim J, Young M, Robey PG, Wang CY, Shi S. 2004. Investigation of multipotent postnatal stem cells from human periodontal ligament. Lancet 364:149–155.

Shimabukuro Y, Ichikawa T, Takayama S, Yamada S, Takedachi M, Terakura M, Hashikawa T, Murakami S. 2005. Fibroblast growth factor-2 regulates the synthesis of hyaluronan by human periodontal ligament cells. J Cell Physiol 203:557–563.
Singh K, DeVouge MW, Mukherjee BB. 1990. Physiological properties and differential glycosylation of phosphorylated and nonphosphorylated forms of osteopontin secreted by normal rat kidney cells. J Biol Chem 265:18696–18701.
Sorensen ES, Petersen TE. 1995. Phosphorylation, glycosylation, and transglutaminase sites in bovine osteopontin. Ann N Y Acad Sci 760:363–366.
Srivatsa SS, Harrity PJ, Maercklein PB, Kleppe L, Veinot J, Edwards WD, Johnson CM, Fitzpatrick LA. 1997. Increased cellular expression of matrix proteins that regulate mineralization is associated with calcification of native human and porcine xenograft bioprosthetic heart valves. J Clin Invest 99:996–1009.
Takahashi F, Takahashi K, Okazaki T, Maeda K, Ienaga H, Maeda M, Kon S, Uede T, Fukuchi Y. 2001. Role of osteopontin in the pathogenesis of bleomycin-induced pulmonary fibrosis. Am J Respir Cell Mol Biol 24:264–271.
Takayama S, Murakami S, Miki Y, Ikezawa K, Tasaka S, Terashima A, Asano T, Okada H. 1997. Effects of basic fibroblast growth factor on human periodontal ligament cells. J Periodontal Res 32:667–675.
Takayama S, Murakami S, Shimabukuro Y, Kitamura M, Okada H. 2001. Periodontal regeneration by FGF-2 (bFGF) in primate models. J Dent Res 80:2075–2079.
Weintraub AS, Schnapp LM, Lin X, Taubman MB. 2000. Osteopontin deficiency in rat vascular smooth muscle cells is associated with an inability to adhere to collagen and increased apoptosis. Lab Invest 80:1603–1615.
Xiao G, Jiang D, Gopalakrishnan R, Franceschi RT. 2002. Fibroblast growth factor 2 induction of the osteocalcin gene requires MAPK activity and phosphorylation of the osteoblast transcription factor, Cbfa1/Runx2. J Biol Chem 277:36181–36187.
Yamada S, Tomoeda M, Ozawa Y, Yoneda S, Terashima Y, Ikezawa K, Ikegawa S, Saito M, Toyosawa S, Murakami S. 2007. PLAP-1/asporin: A novel negative regulator of periodontal ligament mineralization. J Biol Chem 282:23070–23080.
Zohar R, Lee W, Arora P, Cheifetz S, McCulloch C, Sodek J. 1997. Single cell analysis of intracellular osteopontin in osteogenic cultures of fetal rat calvarial cells. J Cell Physiol 170:88–100.
Zohar R, Suzuki N, Suzuki K, Arora P, Glogauer M, McCulloch CA, Sodek J. 2000. Intracellular osteopontin is an integral component of the CD44-ERM complex involved in cell migration. J Cell Physiol 184:118–130.

CD73-Generated Adenosine Restricts Lymphocyte Migration into Draining Lymph Nodes[1]

Masahide Takedachi,*‡ Dongfeng Qu,* Yukihiko Ebisuno,[2†] Hiroyuki Oohara,‡ Michelle L. Joachims,* Stephanie T. McGee,* Emiko Maeda,* Rodger P. McEver,† Toshiyuki Tanaka,§ Masayuki Miyasaka,¶ Shinya Murakami,‖ Thomas Krahn,# Michael R. Blackburn,# and Linda F. Thompson[3]*

After an inflammatory stimulus, lymphocyte migration into draining lymph nodes increases dramatically to facilitate the encounter of naive T cells with Ag-loaded dendritic cells. In this study, we show that CD73 (ecto-5′-nucleotidase) plays an important role in regulating this process. CD73 produces adenosine from AMP and is expressed on high endothelial venules (HEV) and subsets of lymphocytes. *Cd73*$^{-/-}$ mice have normal sized lymphoid organs in the steady state, but ~1.5-fold larger draining lymph nodes and 2.5-fold increased rates of L-selectin-dependent lymphocyte migration from the blood through HEV compared with wild-type mice 24 h after LPS administration. Migration rates of *cd73*$^{+/+}$ and *cd73*$^{-/-}$ lymphocytes into lymph nodes of wild-type mice are equal, suggesting that it is CD73 on HEV that regulates lymphocyte migration into draining lymph nodes. The A_{2B} receptor is a likely target of CD73-generated adenosine, because it is the only adenosine receptor expressed on the HEV-like cell line KOP2.16 and it is up-regulated by TNF-α. Furthermore, increased lymphocyte migration into draining lymph nodes of *cd73*$^{-/-}$ mice is largely normalized by pretreatment with the selective A_{2B} receptor agonist BAY 60-6583. Adenosine receptor signaling to restrict lymphocyte migration across HEV may be an important mechanism to control the magnitude of an inflammatory response. ***The Journal of Immunology*****, 2008, 180: 6288–6296.**

Lymphocyte circulation from the bloodstream to lymph nodes is necessary for immune homeostasis (reconnaissance) under normal physiological conditions and for immune responses against exogenous Ags. This trafficking requires coordinated action of adhesion molecules, chemokines, and chemokine receptors expressed on lymphocytes and high endothelial venules (HEV)[4] (reviewed in Refs. 1 and 2). The interaction of L-selectin with peripheral lymph node addressins (PNAd) initiates lymphocyte tethering and rolling on HEV (3). Chemokine receptor signaling activates the integrin LFA-1 on lymphocytes and induces stable adhesion via binding to ICAM-1 on HEV (4, 5), which is followed by transmigration. The importance of each molecule associated with the entrance of lymphocytes into lymph nodes through HEV has been shown by decreases in lymph node cellularity and defective immune responses in gene-targeted mice (6–10).

TLR signaling activates innate immune responses (reviewed in Ref. 11) in part by inducing APC maturation and recruitment to lymphoid organs via the afferent lymphatics (12, 13). Furthermore, recent reports showed that inflammation induced by a TLR4 or TLR9 agonist controlled naive lymphocyte recirculation in an Ag-independent manner, resulting in an increase in the number of naive lymphocytes in the draining lymph node and an increase in the efficiency of lymphocyte-APC encounters (14). TLR-dependent lymph node hypertrophy was proposed to require vascular growth and arteriole thickening. Although these changes needed at least a few days before they were detectible (14, 15), lymph node growth began within 24 h after a stimulus, implying the existence of other mechanisms that contribute to lymph node swelling. In this study, we present data to show that adenosine (Ado) receptor (AR) signaling, mediated by CD73-generated Ado, plays an important role in regulating early migration of lymphocytes to draining lymph nodes.

CD73 is a 70-kDa GPI-anchored protein with ecto-5′-nucleotidase enzyme activity that catalyzes the dephosphorylation of extracellular nucleoside monophosphates such as AMP to nucleosides such as Ado (16). Extracellular Ado can engage four subtypes of ubiquitously expressed AR (A_1AR, A_{2A}AR, A_{2B}AR, and A_3AR) to modulate a wide array of physiological responses, including vascular tone, neurotransmission, cytokine production, heart rate, and adaptation to hypoxia (reviewed in Ref. 17). In addition to being generated by CD73, Ado can also be generated

*Immunobiology and Cancer Program and †Cardiovascular Biology Program, Oklahoma Medical Research Foundation, Oklahoma City, OK 73104; ‡Department of Periodontology, Division of Oral Biology and Disease Control, Osaka University Graduate School of Dentistry, Osaka, Japan; §Laboratory of Immunobiology, Hyogo University of Health Sciences, Kobe, Japan; ¶Laboratory of Molecular and Cellular Recognition, Osaka University Graduate School of Medicine, Osaka, Japan; ‖Bayer HealthCare, Wuppertal, Germany; and #Department of Biochemistry and Molecular Biology, University of Texas Medical School, Houston, TX 77030

Received for publication April 23, 2007. Accepted for publication March 3, 2008.

The costs of publication of this article were defrayed in part by the payment of page charges. This article must therefore be hereby marked *advertisement* in accordance with 18 U.S.C. Section 1734 solely to indicate this fact.

[1] This work was supported by National Institutes of Health Grants AI18220 (to L.F.T.), P01 HL065607 (to R.P.M.), and AI43372 (to M.R.B.), and was part of the 21st Century Center of Excellence entitled "Origination of Frontier BioDentistry" at Osaka University Graduate School of Dentistry supported by the Ministry of Education, Culture, Sports, Science, and Technology. L.F.T. holds the Putnam City Schools Distinguished Chair in Cancer Research. R.P.M. holds the Eli Lilly Distinguished Chair in Biomedical Research.

[2] Current address: Department of Molecular Genetics, Institute of Biomedical Science, Kansai Medical University, Osaka, Japan 570-8506.

[3] Address correspondence and reprint requests to Dr. Linda F. Thompson, Oklahoma Medical Research Foundation, 825 Northeast 13th Street, Oklahoma City, OK 73104. E-mail address: Linda-Thompson@omrf.org

[4] Abbreviations used in this paper: HEV, high endothelial venule; Ado, adenosine; AR, Ado receptor; CMFDA, 5-chloromethylfluorescein diacetate; CMTMR, 5(and 6)-((4-chloromethyl)benzoyl)amino)tetramethylrhodamine; DC, dendritic cell; PEG, polyethylene glycol; PNAd, peripheral lymph node addressin.

intracellularly through the action of cytoplasmic nucleotidases and then exported via nucleoside transporters. Extracellular Ado has a very short $t_{1/2}$, because it is efficiently taken up into the cytoplasm, where it can be phosphorylated to AMP or degraded to inosine by Ado deaminase. In humans, Ado deaminase can be localized to the cell surface via binding to CD26 (18, 19), giving it the potential to inhibit AR signaling through deamination of extracellular Ado (20). Mice deficient in the expression of each AR have been engineered and characterized (21–25). Each strain has a variety of interesting phenotypes, revealing the diverse consequences of AR signaling. However, the mechanism by which extracellular Ado levels are regulated to modulate AR engagement in vivo is not fully understood.

Ado is a well-known anti-inflammatory mediator (26). Recent studies clearly showed that CD73 makes a major contribution to the generation of extracellular Ado in a number of physiologically relevant experimental models and plays a critical role in host defense systems. For example, CD73 attenuates hypoxia-induced vascular leakage, FMLP-stimulated neutrophil adhesion to endothelial cells, and neutrophil accumulation in tissues (27–29). Furthermore, *cd73*-deficient mice are susceptible to vascular inflammation and neointima formation due to decreased concentrations of endogenous Ado (30). CD73 deficiency increases VCAM-1 expression on endothelial cells isolated from carotid arteries through NF-κB activation; however, ICAM-1 expression is unchanged. This proinflammatory phenotype of *cd73*-deficient endothelium causes the arrest of monocytes and exacerbates wire-induced injury.

These observations demonstrated a crucial role for CD73-generated Ado in the interaction of myeloid cells with vascular endothelium. However, the in vivo function of this molecule in lymphocyte-endothelium cross-talk remains unclear. In addition to its enzymatic role in the production of extracellular Ado, CD73 has also been characterized as a signaling molecule (31) and an adhesion molecule (32). Engagement of lymphocyte CD73 with anti-CD73 mAbs has been shown to stimulate proliferation, IL-2 secretion, and IL-2R expression (33, 34). Furthermore, blocking this molecule on lymphocytes with an Ab appears to inhibit adhesion of lymphocytes to cultured endothelial cells (35). Thus, there are multiple mechanisms by which CD73 could impact lymphocyte migration across HEV. We show in this study that *cd73*-deficient mice have increased rates of lymphocyte homing to draining lymph nodes, and propose that CD73-generated Ado regulates the ability of lymphocytes to migrate across HEV, thus limiting their access to inflamed lymph nodes.

Materials and Methods

Mice

Cd73-deficient mice developed in our laboratory (27) were backcrossed onto C57BL/6J for 14 generations. Genotyping by PCR, using primers that differentiate between the wild-type *cd73* allele and the mutated *cd73* allele containing a neomycin resistance cassette, was performed, as previously described. $A_{2B}AR^{-/-}$ mice were obtained from Deltagen and have also been backcrossed onto the C57BL/6 background. All mice were bred and maintained in our animal facility under specific pathogen-free conditions. All protocols were approved by the Oklahoma Medical Research Foundation Institutional Animal Care and Use Committee.

Cell culture

The cell line KOP2.16 was derived from stromal cells taken from pooled mouse lymph nodes and has been described previously (36). It was cultured in DMEM supplemented with 20% FCS (HyClone), 10 mM HEPES, 1 mM sodium pyruvate, 2 mM L-glutamine, 5×10^{-5} M 2-ME, nonessential amino acids, 100 U/ml penicillin, and 100 μg/ml streptomycin. In some experiments, 20 ng/ml TNF-α (R&D Systems) was added for 3–6 h.

Cd73 *and AR gene expression*

Cd73 and AR expression were analyzed by PCR in a full-length cDNA library derived from MACS (Miltenyi Biotec)-isolated $PNAd^+$ endothelial cells from lymph nodes (37) using previously described primers (38). In other experiments, RNA was prepared from KOP2.16, and RT-PCR was performed as described using β-actin as an internal control (38).

Digestion of lymph nodes for characterization of HEV or enumeration of $CD11c^+$ dendritic cells (DC) by flow cytometry

Lymph nodes were dissected from mice, minced with scissors, and digested in RPMI 1640 containing 10% FCS, 1 mg/ml collagenase B (Roche), and 2 μg/ml DNase I (Roche) for 30 min at 37°C with shaking at 50 rpm. The cell suspension was passed through a Pasteur pipette 40 times, followed by digestion with 0.2% trypsin (Mediatech) and 0.5 mM EDTA at 37°C for 10 min. Cells were then passed through a 70-μm filter, washed, and stained.

Immunofluorescence

Lymphoid cells or $PNAd^+$ cells were stained with the following mAbs: FITC anti-CD4, FITC anti-CD8, FITC anti-MHC class II, PE anti-CD11c, PE-Cy5.5 anti-CD19, and allophycocyanin anti-CD45R (Caltag Laboratories); PE anti-TCRβ (BD Pharmingen); allophycocyanin anti-CD45 (Southern Biotechnology Associates); and biotinylated anti-CD73 (TY/23) (39), according to standard methods. PE-streptavidin was from BD Pharmingen. Data were collected with a FACSCalibur (BD Biosciences) and analyzed with CellQuest software. For lymphocyte migration experiments and experiments to enumerate DC, data were collected on 750,000 and 350,000 cells, respectively.

Immunohistochemistry

Frozen sections (7 μm) of lymph nodes were fixed with cold acetone and blocked with 3% BSA in PBS. Sections were stained with TY/23 (anti-CD73, IgG2a), followed by Alexa Fluor 488-conjugated donkey anti-rat IgG (Molecular Probes), and then blocked with purified mouse IgG at 500 μg/ml. After washing, they were then stained with Alexa Fluor 594-conjugated anti-PNAd mAb MECA-79 (IgM; BD Pharmingen). Other slides were stained with a combination of TY/23 and rabbit anti-collagen IV (Chemicon International), followed by a combination of Alexa Fluor 488-conjugated donkey anti-rat IgG plus Alexa Fluor 594-conjugated donkey anti-rabbit IgG (Molecular Probes).

Inflammatory stimuli

Anesthetized mice were injected with 1 μg of *Escherichia coli* LPS (055:B5; Sigma-Aldrich) or 5 μg of poly(I:C) (Sigma-Aldrich) in 30 μl of PBS in the left front footpad using an insulin syringe. The right footpad was injected with same volume of PBS. Twenty-four hours later, brachial lymph nodes were examined as draining lymph nodes. In other experiments, mice were injected in either the rear footpad or thigh, and popliteal or inguinal lymph nodes, respectively, were studied as draining lymph nodes.

Lymphocyte homing assay

Total splenocytes were labeled with 0.25 μM 5-chloromethylfluorescein diacetate (CMFDA; Molecular Probes) for 30 min at 37°C. Ten million labeled cells were injected i.v. into mice, and 1 h later, spleen and lymph nodes were harvested. In some experiments, *cd73*-deficient and wild-type splenocytes were labeled with 0.25 μM CMFDA and 2 μM 5(and 6)-((4-chloromethyl)benzoyl)amino)tetramethylrhodamine (CMTMR; Molecular Probes), respectively, for 30 min at 37°C. Equal numbers of labeled cells were coinjected i.v. into both strains of mice. Harvested lymph nodes were pushed through 70-μm filters to make single-cell suspensions. Cells were then counted, and the percentages of labeled cells were determined by flow cytometry. In selected experiments, anti-L-selectin Ab (MEL-14; Southern Biotechnology Associates) was given to mice (50 μg/mouse i.v.) simultaneously with LPS. In other experiments, mice were pretreated with the $A_{2B}AR$ agonist BAY 60-6583 (40) at 0.32 mg/kg (Bayer HealthCare; dissolved in polyethylene glycol (PEG) 400 and diluted to 80 μg/ml in PBS for i.v. injection) 30 min before the injection of labeled splenocytes.

Results

CD73 and AR expression in lymphoid tissues and HEV

We previously reported the expression pattern of CD73 in lymphoid tissues of BALB/c mice (39); however, experiments indicating that CD73 expression was strain dependent prompted us to

investigate CD73 expression in lymphoid cells of C57BL/6 mice before using this strain for the experiments described in this study. Staining with mAb TY/23 revealed that ~50% of $CD4^+$, 85% of $CD8^+$, and 2% of $CD19^+$ lymphocytes derived from lymph nodes of wild-type mice expressed CD73 (Fig. 1*A*). We confirmed the findings of Kobie et al. (41) that CD73 is expressed on $CD4^+CD25^+Foxp3^+$ regulatory T cells. Nevertheless, $cd73^{+/+}$ and $cd73^{-/-}$ mice had similar proportions of T cells with this phenotype (data not shown). Lymphocytes from $cd73^{-/-}$ mice expressed no detectable CD73, confirming the deletion. We also analyzed CD73 expression on HEV by flow cytometry, gating on the rare population of $CD45^-$ $PNAd^+$ cells (0.05–0.15% of cells from enzyme-digested whole lymph nodes). Relatively high CD73 expression was observed on HEV compared with lymphocytes (Fig. 1*B*). To substantiate the results, immunohistochemistry was performed (Fig. 1*C*). Sections stained with anti-PNAd Ab and TY/23 revealed that HEV expressed CD73 abundantly. In contrast, only a few lymphocytes expressed enough CD73 to be detectable by this method. In addition, double staining with anti-collagen IV Ab and TY/23 demonstrated that CD73 is also expressed homogeneously on basal lamina (i.e., not polarized to the luminal or abluminal surface).

Steady-state mRNA levels of *cd73* and the AR were measured in HEV by PCR, using a cDNA library derived from $PNAd^+$ endothelial cells (Fig. 1*D*). *Cd73* and $A_{2B}AR$ were detected, but A_2AR, $A_{3}AR$, and A_3AR were not expressed at detectible levels. Steady-state levels of AR mRNA in murine splenocytes are shown in Fig. 1*E*. All AR except the A_1AR were easily detected.

CD73-deficient mice have large draining lymph nodes

CD73 has been proposed to modulate lymphocyte-endothelial cell interactions as an adhesion molecule (32, 35). Therefore, we asked whether CD73 plays a role in lymphocyte homing to secondary lymphoid tissue in the steady state. The sizes of spleen, peripheral lymph nodes, Peyer's patches, and mesenteric lymph nodes in *cd73*-deficient mice were normal (27 and our unpublished data). Furthermore, the migration of CMFDA-labeled $cd73^{-/-}$ splenocytes to lymphoid tissues (spleen and lymph node) of unmanipulated $cd73^{-/-}$ mice was also comparable to that of $cd73^{+/+}$ splenocytes to lymphoid organs of unmanipulated wild-type mice (our unpublished data). These observations suggested that CD73 does not have an obvious function in lymphocyte homing under steady-state conditions.

CD73 plays important roles in vivo in maintaining the integrity of the vascular endothelium during hypoxia (27–29) and in regulating endothelial adhesion molecule expression after wire-induced injury (30). Taking this information into account, and considering the well-known anti-inflammatory properties of Ado, we hypothesized that CD73 might also regulate lymphocyte-HEV interactions after an inflammatory stimulus. To address this issue, LPS was injected into front left footpads of $cd73^{+/+}$ and $cd73^{-/-}$ mice, and 24 h later, the brachial (draining) lymph node cellularity was examined (Fig. 2*A*). The same volume of PBS was administered to the contralateral side as a control. As expected from previous studies (14, 15), the draining lymph nodes were dramatically enlarged compared with those on the control side in wild-type mice. Consistent with our hypothesis, there was a further increase in the size of the draining lymph nodes from *cd73*-deficient mice, which were 1.5-fold larger than those of wild-type mice. To examine whether lymphocyte migration from the bloodstream to lymph nodes is also accelerated in $cd73^{-/-}$ mice, CMFDA-labeled wild-type splenocytes were injected i.v. 24 h after LPS injection and the accumulation of labeled cells in the lymph nodes was measured after 1 h by flow cytometry (Fig. 2*B*). Although no differences were observed between $cd73^{+/+}$ and $cd73^{-/-}$ mice on the control side, the number of lymphocytes that migrated into the draining lymph nodes of *cd73*-deficient mice was 2.7-fold greater than in

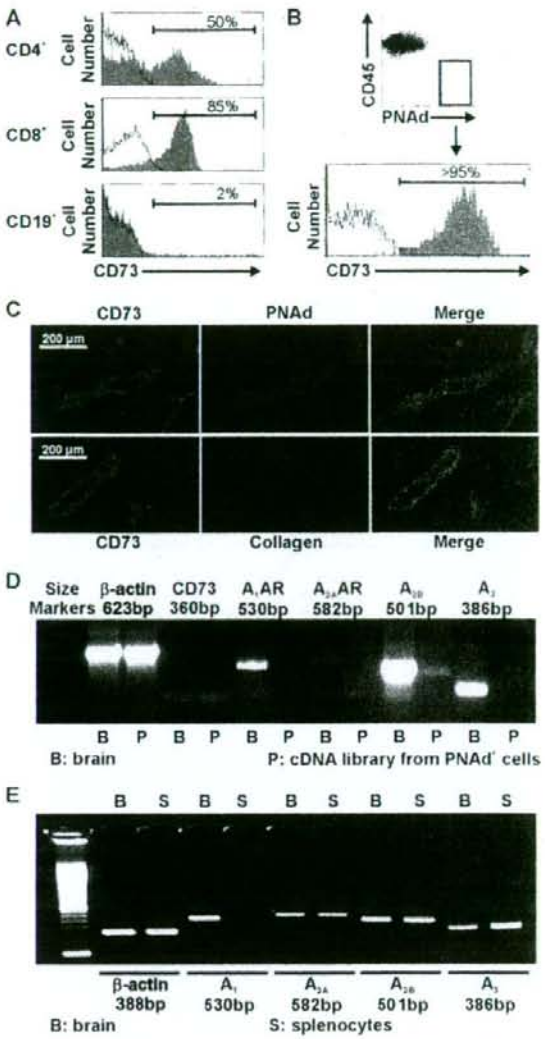

FIGURE 1. CD73 expression on lymphocytes and HEV. *A*, Single-cell suspensions of lymph node cells from $cd73^{+/+}$ and $cd73^{-/-}$ mice were stained with FITC anti-CD4, FITC anti-CD8, or PE-Cy5.5 anti-CD19 plus biotinylated anti-CD73 (TY/23) and PE-streptavidin or the relevant isotype-matched control Abs. CD73 expression in $cd73^{+/+}$ mice is shown in the shaded histograms, and that in $cd73^{-/-}$ mice is shown with solid lines. Staining with isotype control Abs is shown with dotted lines. The dotted lines and solid lines are virtually overlapping. *B*, Other lymph nodes from wild-type mice were digested with collagenase, DNase I, and trypsin, as described in *Materials and Methods*, and cells were stained with allophycocyanin anti-CD45, purified anti-PNAd plus Alexa Fluor 488 anti-IgM, and biotinylated anti-CD73 plus PE-streptavidin. HEV were identified as $CD45^-$ $PNAd^+$ cells. *C*, Frozen sections of lymph nodes were stained with anti-CD73 (TY/23) and either anti-PNAd or anti-collagen IV, as described in *Materials and Methods*. *D*, *Cd73* and AR expression were assessed by RT-PCR in a cDNA library derived from $PNAd^+$ endothelial cells. Representative results are shown from more than three experiments. *E*, AR expression was assessed by RT-PCR in total wild-type splenocytes. Representative results from more than three experiments are shown.